CASE WESTERN RESERVE UNIVERSITY

SCHOOL OF DENTISTRY

GRADUATE STUDIES

We hereby approve the thesis of

Sean Patrick Bates

candidate for the degree Master of Science

in Dentistry.

Signed: _____ (Chairman)

_____

_____

_____

_____

Date: October 15th, 2003

NON-DESTRUCTIVE DETERMINATION OF THE CORRELATION OF SKULL RADIODENSITY TO STIFFNESS AND STRENGTH IN A FRESH-FROZEN CADAVER

Abstract

by

SEAN PATRICK BATES

The purpose of this study was to determine whether radiodensity data obtained by CT-scan could be used to accurately predict the material properties of a patient's skull. If radiodensity is sufficiently correlated with stiffness and strength it could be used to predict a craniofacial finite element model capable of simulating a patient's response to surgical or appliance treatment including the possibility of skeletal failure. The skull and mandible of a 75 year old female was obtained as a fresh-frozen cadaver specimen. The protocol began with defleshing and 3D CT-scanning of the skull. Using a craniostat, a 1 x 1 cm grid was drawn on the skull and 77 bone sample sites were selected along with 6 teeth. Samples were sectioned using a Dremel™ drill mounted with a sectioning disk. The samples were then flattened using

a CNC device and manually polished. The mass-density of each piece was determined using an OHAS Adventurer™ electronic scale for mass and a 25ml KIMAX™ graduated cylinder for volume displacement. The stiffness properties of each piece were determined with an Olympus UH3™ scanning acoustic microscope. Stiffness was measured as the acoustic impedance of the external cortical bone surface. Strength properties were determined via a microindention Vicker's hardness test which measures the surface fracture that results when a known force projected into the external cortical bone surface. A CT-scan of the isolated bone pieces and teeth allowed calculation of radiodensity. The process of voxel segmentation removed artifact and corrected for partial volume error. The data showed that the material properties of stiffness and strength, varied across the craniofacial complex. Positive correlations were found between radiodensity and stiffness ($r = 0.47$) and radiodensity and strength ($r = 0.24$).

DEDICATION

To Anita, my wife, thank you for your endless love and enduring support throughout this residency. I promise that our hearts to be alone and heavy no longer again.

To my mother and father, thank you for all the love, support, opportunities you provided in order to make my dreams come true. The qualities that you both instilled in me have made me the person that I am today.

ACKNOWLEDGEMENTS

Dr. David Dean provided knowledge, support, and guidance as thesis director, guiding this project to a successful completion.

Dr. Robert Mullen provided the expertise in the area of biomechanics making sure the project provided valuable results for future studies.

Dr. Mark Hans provided leadership as chairman and assisted in guiding the project to completion.

Dr. Martin Palomo provided computer expertise which assisted in the graphics and stats.

Tae Jung provided instruction in use all aspects of this project and often worked tirelessly to see this project to completion.

Dr. Clare Rimnac and Rebecca Thomas provided use of the Wearn wet lab and CNC.

Dr. Steven Eppell and Dr. Lawrence Katz provided guidance in the operation of the scanning acoustic microscope.

Dr. Mark Deguire provided use of the microindenter.

Liz Russel and Les Ciancibello provided their expertise in the use of CT scanner at University Hospital.

June Min and Eric Hu provided computer knowledge for partial volume correction.

Dr. B. Holly Broadbent, Jr. provided the craniostat used to grid the skull.

Dr. Stan Hirsh provided valuable insight into the formatting and preparation of this thesis.

Case Western Reserve School of Dental Medicine provided the monetary support, freezer, and additional supplies used in the project.

The Orthodontic Department Staff helped make my residency pleasant and productive.

All my classmates Drs. David Lenhart, Lance Bruntz, and Chris Spoonhower, made the last two years both memorable and enjoyable. My friends and family who were always there for me.

TABLE OF CONTENTS

	Page
ABSTRACT	ii
DEDICATION	iv
ACKNOWLEDGEMENTS	v
TABLE OF CONTENTS	vii
LIST OF FIGURES	x
LIST OF TABLES	xii
Chapter	
1. INTRODUCTION	1
1.1 What Determines Treatment Effect?	1
2. LITERATURE REVIEW	3
2.1 Craniofacial Stress-Strain Models	3
2.2 Earliest Bone Finite Element Models	4
2.3 The Limits of Homogeneous Skull Material Property Assumptions	5
2.4 Measuring the Material Properties of Bone	6
2.5 Linking Bone Material Properties to CT derived Radiodensity	8
2.6 Correlating Radiodensity to the Material Properties of Bone	9

Page

2.7 A Bovine Pilot Study..... 11

2.8 The Dry Skull Project..... 11

3. HYPOTHESES..... 13

4. MATERIALS AND METHODS..... 14

4.1 Specimen Acquisition and Gross Preparation for Biomechanical Study..... 14

4.2 External Skull Surface Gridding, Cutting, and Fine Bone Preparation for Density, SAM, and Microindentation Data Collection..... 15

4.3 Mass Density Recording..... 27

4.4 Scanning Acoustic Microscopy..... 28

4.5 Microindentation..... 31

4.6 Isolated Piece CT Scanning..... 34

4.7 Segmentation..... 35

4.8 Statistical Analysis..... 38

5. RESULTS..... 40

5.1 Summary Data Table..... 40

5.2 Correlation between Radiodensity and Stiffness..... 45

5.3 Correlation between Radiodensity and Strength..... 46

6. DISCUSSION..... 48

6.1 Methodological Observations..... 48

6.2 Summary of Materials and Methods..... 54

Page

6.3 Regional Results..... 54

6.4 Summary of Material Properties..... 61

7. CONCLUSIONS..... 63

APPENDIX: Raw Data for Mass Density of Bone Pieces and Teeth..... 64

Raw Data for Scanning Acoustic Readings of Bone and Teeth..... 69

Raw Data for Vicker's Hardness for Bone Pieces and Teeth..... 99

Raw Data Values for Cortical Bone and Teeth..... 115

BIBLIOGRAPHY..... 117

LIST OF FIGURES

Figure		Page
1	Gridding	15
2	Craniostat	16
3	Norma Frontalis Gridding Scheme	18
4	Norma Occipitalis Gridding Scheme	19
5.	Right Norma Lateralis Gridding Scheme	20
6.	Left Norma Lateralis Gridding Scheme	21
7	Norma Superioris Gridding Scheme	22
8	Norma Basalis Gridding Scheme	23
9	Right Mandibular Gridding Scheme	24
10	Left Mandibular Gridding Scheme	25
11	Instruments Used in Skull Sectioning	26
12	Bone Micro-Machining Device	27
13	Scanning Acoustic Microscope (SAM)	28
14	SAM Specimen Mounting	29
15	Sampling Pattern for the Scanning Acoustic Microscope	30
16	Mounting of Bone Sample on Acrylic Base	31
17	Instruments and Materials for Basing of Specimen for Microindentation	32

Figure Page

18 Microindenter..... 33

19 Diamond head Impressions from Microindenter.... 33

20 Bone Piece and Base Pre-Segmentation..... 36

21 Bone Piece Post Segmentation..... 37

22 Radiodensity vs. Stiffness..... 46

23 Radiodensity vs. Vicker's Hardness..... 47

LIST OF TABLES

Table		Page
1	Visual Key for Mid and Upper Face. Bone and maxillary tooth sample numbers (1-18 and maxillary teeth)	18
2	Visual Key for Norma Occipitalis. Bone sample numbers (30-36)	19
3	Visual Key for Right Norma Lateralis. Bone sample numbers (40-47)	20
4	Visual Key for Left Norma Lateralis. Bone sample numbers (50-57)	21
5	Visual Key for Norma Superioris. Bone sample numbers (20-26)	22
6	Visual Key for Norma Basalis. Bone sample numbers (60-65)	24
7	Visual Key for Right Mandibular Bone and Teeth. Bone and tooth sample numbers (70-77 and mandibular teeth)	25
8	Visual Key for Left Mandibular Bone. Bone sample numbers (80-87)	25
9	Summary Data Table. Data summary for the Material Properties of Density, Stiffness, and Strength for the Craniofacial Complex of Fresh-Frozen Cadaver Bone	42
10	Raw Data for Mass Density of Bone Pieces and Teeth	64

11 Raw Data for Scanning Acoustic Microscope Readings of Bone and Teeth..... 69

12 Raw Data for Vicker's Hardness (H_v) for Bone Pieces and Teeth..... 99

13 Raw Data for Radiointensity Values for Cortical Bone and Teeth..... 115

1. INTRODUCTION

1.1 What Determines Treatment Effect?

Therapeutic manipulation of the craniofacial skeleton by appliance, prosthetic, and/or surgery is commonly preceded by image-based treatment planning. Information regarding normal patterns of craniofacial development (Dean et al. 2000) and adult form (Subramanyan and Dean 2000) are commonly incorporated into manual (Broadbent 1931) or electronic (Hans et al. 2001) comparisons of normative and patient images. The resulting treatment plan may include a morphological analysis allowed by these images, but not the mechanical effects that treatment is expected to have on the patient. While a great deal is known about the mechanical properties of appliances and prosthetic implants, there is very little known about the biomechanical response (i.e., expected stress-strain relationships) of the craniofacial skeleton to treatment (Mullen and Rudderman 1992). Understanding the biomechanical effect of treatment on the craniofacial

complex can influence treatment choices or treatment protocol. For example, the success of procedures that depend upon the conveyance of forces through specific craniofacial locations should also be characterized by the amount and location of effective force. The timing and duration of such treatments/procedures could be influenced by the "treatment responsive periods" of adolescence. Additionally, it is possible that, in some patients, "therapeutic" stress-strain relationships will be found to cause bone mortality or fracture from biomechanical overload and should, therefore, be avoided. Orthodontics, orthopedics, otolaryngology, plastic surgery, neurosurgery, ophthalmology, prosthodontics and oral surgery, are some of the medical fields that could benefit from such knowledge.

2. LITERATURE REVIEW

2.1 Craniofacial Stress-Strain Models

The clinical significance of craniofacial stress-strain patterns has been suggested for nearly a century. In the 1920's, one of the first craniofacial biomechanical models described occlusal forces dissipating through three major trajectories: maxillonasal, maxillozygomatic and maxillopterygoid (Sicher and Tandler 1928). Conceptual models developed since then have attempted to describe strain trajectories in terms of pillars, buttresses, triangles, pyramidal trusses, and lever systems based on mechanical and architectural analogies, functional bone adaptation, split-line patterns and strain gauge data (Tappen 1953; Couly 1976; Hylander 1975, 1984, 1985; Hylander et al. 1991). Many of these hypothetical models have been proposed as explanations of stress-strain relationships during normal activity. The majority of simulations used to test these models have assumed that cranial bone has homogeneous material properties. However, work on the

stress-strain models of the femur and tibia have called these assumptions into question (Keyak et al. 1993). More recently, high resolution shape information for human bone has been used to create Finite Element Models (FEMs) of stress-stain distributions which are starting to include the craniofacial complex (Gross et al. 2001; Cattaneo et al. 2003; Jafari et al. 2003).

2.2 Earliest Bone Finite Element Models

Since the early 1970's finite element models have been presented as simulations of the reactions of bone to physiological and non-physiological load conditions (Wirtz et al. 2000). The earliest finite element model of the human skull based on computed tomography (CT) was presented by Arbel (1993). However, one of the shortcomings in the creation of these early finite element models was the assumption of isotropic and homogeneous bone material properties (Meijer et al. 1993). Although the assumption of isotropic and homogeneous properties allows for the fabrication of finite element models, it must also be regarded as a shortcoming if the craniofacial complex actually has heterogeneous material properties. In that case, homogeneous material properties would fail to find local

correlations between geometry or density in different regions of craniofacial complex (Gross et al. 2001).

2.3 The Limits of Homogeneous Skull Material Property Assumptions

One of the reasons for this assumption has been a difficulty in measuring the material properties of human craniofacial bone. Bone in this region varies tremendously in thickness, density, anatomic complexity and topography (Gross et al. 2001). The majority of instruments capable of material property testing require samples with ideal shapes (e.g., cylinders, cubes, etc.) and flat surfaces. However, it is difficult to map and cut this bone so that one repeatedly obtains homologous segments for testing from different individuals. Additionally, many studies have used desiccated specimens without also surveying fresh (i.e., physiological conditions) bone (Jafari et al. 2003). If one attempts to systematically map, cut and sample material properties from fresh cranial bone, maintaining the *in vivo* condition of the bone segments requires avoidance of post-mortem degradation.

Work on the skull and mandible is not only limited by the complexity of specimen preparation, but also, the

expense of specimens. These constraints have usually resulted in studies with low sample size (Dabney and Dechow 2003). Studies of the material properties of the craniofacial complex have primarily focused on the cortical bone of the mandible (Ashman and Van Buskirk 1987; Arendts and Sigolotto 1990; Dechow et al. 1993, 2003) with the midface and cranium proper receiving limited investigation (Peterson and Dechow 2002). Thus, study of material property variation, across the cranium and mandible has received little systematic study (Dabney and Dechow 2003).

2.4 Measuring the Material Properties of Bone

2.4.1 Destructive Methods For Measuring Stiffness and Strength

The current methods for acquiring material properties require samples that have simple geometries. Stiffness or strength can be calculated from Instron-based three or four-point bending or compression tests. However, the acquisition of material properties by these methods comes at the expense of the bone sample. The sample prepared to be measured in the device is destroyed in the process along with the ability to test radiodensity, or to repeat or continue testing the piece

to insure methodological precision. In order to continue testing, additional samples need to be located, purchased and prepared, requiring additional time and expense. A nondestructive method of acquiring these material properties would more reliable because the readings could be repeated.

2.4.2 Nondestructive Determination of Bone Quality

Nondestructive determination of bone material properties should allow:(1) multiple testing at the same location on the same sample from the same individual; (2) repeat measurements that test methodological precision; and, (3) resolution that is adequate (i.e., not too coarse or too fine). The scanning acoustic microscopic (SAM) and the microindentator allow for the repeatable nondestructive gathering of material properties, both stiffness and strength, from a single piece of bone.

2.4.2.1 Ultrasonic Testing

The SAM measures the stiffness of a material based on the rate that ultrasonic sound waves travel through it. This rate is dependent upon the specimen's elastic properties and its density. Sound velocity can be measured by transmitting a wave through a specimen and measuring this sound transduction on an oscilloscope as

the time required for the wave to traverse the specimen; the width of the specimen divided by the time delay will determine the sound wave's velocity (Yoon and Katz 1976; Ashman et al. 1987; Turner and Eich 1991). The nondestructive nature of ultrasonic testing leaves the biological material unaltered and available for strength and/or radiodensity testing.

2.4.2.2 Microindenter

Strength is measured as the ability to resist indentation (crushing) or penetration (fracture). A miroindenter produces a tiny impression in the material tested using a specified load and indenter size. The Vicker's hardness value measures the hardness of the material based upon the size of the impression produced under a specified load applied through a pyramid shaped diamond indentor. This test was devised in the 1920's by engineers at Vicker's Ltd., London, England.

2.5 Linking Bone Material Properties to CT derived Radiodensity

If CT density (radiodensity) were shown to correlate highly with cranial and mandibular strength and stiffness, it should be possible to use the density information in a 3D CT scan to accurately predict the

information in a 3D CT scan to accurately predict the material properties of a patient's skull. This possibility is the primary motivation for the current study.

2.6 Correlating Radiodensity to the Material Properties of Bone

The use of radiodensity to represent the material properties of bone has previously gained particular attention in the area of research into osteoporosis (Lai et al. 1993; Sato 1995; Keenan et al. 1997; Ulrich et al. 1999). Osteoporosis research has focused on *in vivo* monitoring of the density of bone through biopsy densitometry procedures. The standard procedure for bone density measurements has historically relied on Archimede's principal for density measurements (i.e., the bone's mass divided by the volume of water it displaces). Although this procedure is extremely accurate, it does require a biopsy to obtain the necessary sample for testing purposes. This biopsy is not only invasive, but only represents the density of a very specific site.

More recently bone density has been determined non-invasively using dual-energy X-ray absorptiometry (DXA). In a 1994 article, Sievanen *et al.* determined that DXA

was a precise tool to for measuring bone mineral density and bone mineral content. This determination allowed for a comparison study between the clinical utility of bone densities obtained by DXA and Archimedies' principle (Keenan 1997). Results from the study determined that there was a strong correlation between the Archimedies' principle and DXA (r = 0.82)(Keenan 1997). For more than a decade, DXA has proven to be a reliable tool for clinical bone analysis (Sato 1995).

The development of quantitative computed tomography (QCT) has provided another tool for densitometric analysis of bone. In 1995, Sato conducted a bone x-ray densitometry comparison between DXA and QCT. Bone density from the proximal tibiae of shams and ovariectomized rats were evaluated. Compared to DXA, QCT has a higher resolution and is able to measure volumetric mineral density (mg/cc). Precision and accuracy analysis between the two techniques has shown that QCT was better suited for the analysis of small bone samples (e.g., 1.04-9.6 mm) (Sato 1995).

Studies of fresh bone to date have found weak to moderate correlation between modulus values and CT values (r = 0.52) (Lettry et al. 2003).

2.7 A Bovine Pilot Study

A new method to correlate radiodensity with stiffness and strength, as determined by SAM and microindenter, in a single piece of bone has been recently developed at Case Western Reserve University (Dean et al.). In a pilot study, Dean et al. used five fresh-frozen bovine (cow) crania to determine mass and radio-density. The goal of this work was to obtain both the geometry and material properties for a three dimensional finite element model from a 3D CT-scan. This bovine pilot study was successful in demonstrating the significant difference between assumptions of homogenous material properties and actual values. In addition, positive correlations were established between stiffness and radiodensity and strength and radiodensity. However, there are significant architectural, histological, and material property differences between bovine and human skulls. It is, therefore, necessary to test these correlations in human cranial materials.

2.8 The Dry Skull Project

Dr. Dean's laboratory extended the methods used above with bovine specimens to a desiccated (dry) human skull (Jung et al. 2003). The samples tested had enough

externally oriented compact bone to undergo micromachining and polishing that resulted in flat surfaces. This project used a craniostat (Figure 2) to grid the entire external skull. Over eighty pieces of bone were selected from the frontal, parietal, temporal, occipital, maxilla and mandible from both sides of the skull.

3. HYPOTHESES

The present study plans to determine the homogeneity of the material properties of mass density, stiffness, and strength of the human craniofacial complex. If these properties are heterogeneous, a second objective will be to determine the correlations between bone and tooth material properties (mass density, stiffness, and strength) and radiodensity.

The present study has the following hypotheses:

1. The material properties of the skull specimen will show significant variation across the entire craniofacial complex.

2. There will be a positive correlation between radiodensity and both stiffness and strength of the skull.

4. MATERIALS AND METHODS

4.1 Specimen Acquisition and Gross Preparation for Biomechanical Study

A fresh-frozen cadaver was obtained from the Mortuary of the School of Medicine at Case Western Reserve University. The specimen was a 75-year-old female who's cause of death (cancer) had not involved wasting nor had it impacted the integrity of her craniofacial complex. Gross preparation commenced with decapitation of the cadaver and removal of the brain through the foramen magnum. The craniofacial complex was then defleshed with particular care to remove the periosteum without damaging the underlying bone. This task was accomplished using #10 surgical scalpels and periosteal elevators to reflect tissue from the bone without damaging the bone itself.

The defleshed cranial material was then wrapped in wet muslin and placed into airtight plastic freezer bag and frozen at -4° Celsius. A 3D-CT scan of the defleshed frozen skull was taken using a Siemens Somatom Plus Four™

scanner. This 3D CT scan was taken with 2 mm slice thickness at 140 kV and 111 mA.

4.2 External Skull Surface Gridding, Cutting, and Fine Bone Preparation for Density, SAM, and Microindentation Data Collection

A grid was drawn on the thawed skull with indelible marker in 1 x 1 cm portions to serve as cut lines for subsequent processing into smaller samples (Figure 1).

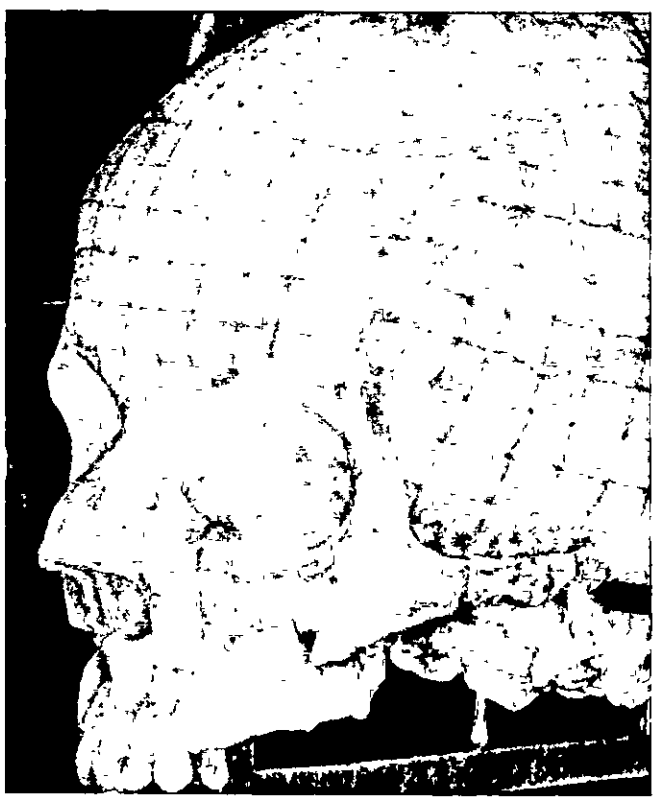


Figure 1. Gridding. The skull was gridded in 1 x 1 cm sections with indelible marker grided by a craniostat.

A craniostat was kindly provided by the Bolton-Brush Growth Study at the CWRU School of Dental Medicine. It was used to guide the pen during gridding (Figure 2).

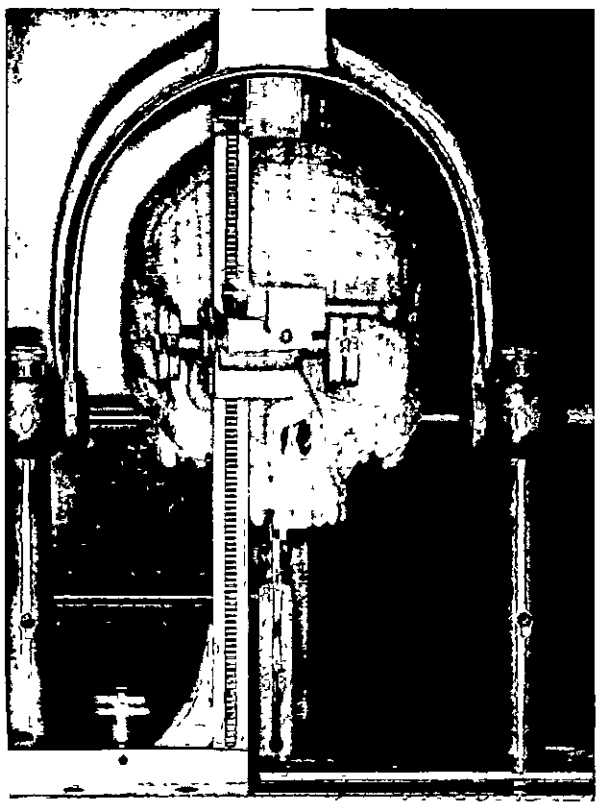


Figure 2. Craniostat. Used for gridding the skull in 1 x 1 cm sections.

The skull was placed in the craniostat with the ear rods extending into both exteral acoustic meatuses. Gridding was started parallel to the mid-saggital suture. Sagittal lines were drawn beginning anteriorly and moving posteriorly, from the frontal to the parietal bone.

Completion of the sagittal lines required rotation of the skull in the craniostat along its frontal axis. Once the anterior-posterior lines were completed the skull was removed from the craniostat and rotated 90°. Securing the skull into the craniostat was accomplished using the ear rods and the craniostat's stage as support. Coronal lines were drawn to complete the grid. During the process of gridding, the skull was moistened every fifteen minutes with distilled pH 7 water. Upon completion the skull was wrapped with muslin soaked in distilled pH 7 water and placed in an airtight bag in preparation for sectioning. Sections chosen for mechanical testing were taken from the same location on both sides of the skull, sampling the: frontal, parietal, temporal, occipital, maxilla, and mandible. Bone sample locations were selected to have sufficiently flat surfaces of externally oriented compact bone thick enough to sustain micro-machining and polishing. Piece locations were also selected in order to evenly sample the entire external skull surface. Selection of the sample sites was aided by the similar study of a desiccated human skull by Jung et al., (2003). Sixteen bone samples and three maxillary teeth (one incisor, one

canine and one premolar) were collected from the midface-maxillary region (Figure 3).

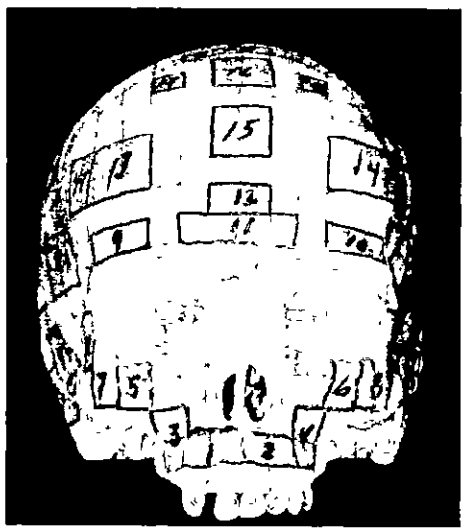


Figure 3. Norma Frontalis Gridding Scheme

In the tables 1-8 symmetrical refers to present on the right and left sides, whereas asymmetric refers to present only in the midline.

TABLE 1.-- Visual Key for Mid and Upper Face. Bone and maxillary tooth sample numbers (1-18 and maxillary teeth).

Tooth/bone sample #	Symmetrical/Asymmetrical	Sample Location (Bone)
1,2,3,4, *maxi,*maxc*,maxp	Symmetrical	Maxilla
5,6,7,8	Symmetrical	Zygomatic
9,10,13,14,17,18	Symmetrical	Frontal
11,12,15,16	Asymmetrical	Frontal

*maxi – maxillary incisor, *maxc – maxillary canine, *maxp - maxillary premolar

Seven bone samples were selected from the occipital region (Figure 4).

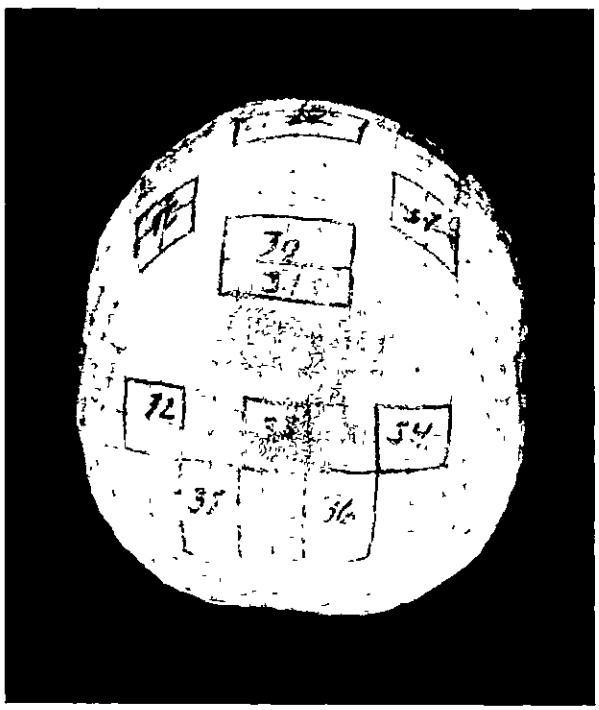


Figure 4. Norma Occipitalis Gridding Scheme.

The samples were representative of both the parietal and occipital bones (Table 2).

TABLE 2.– Visual Key for Norma Occipitalis. Bone sample numbers (30-36).

Tooth/sample #	Symmetrical/Asymmetrical	Sample Location (Bone)
30,31	Asymmetrical	Parietal
33	Asymmetrical	Occipital/Parietal
32,34	Symmetrical	Parietal
35,36	Symmetrical	Occipital

From right norma lateralis view eight sample regions were chosen for testing (Figure 5).

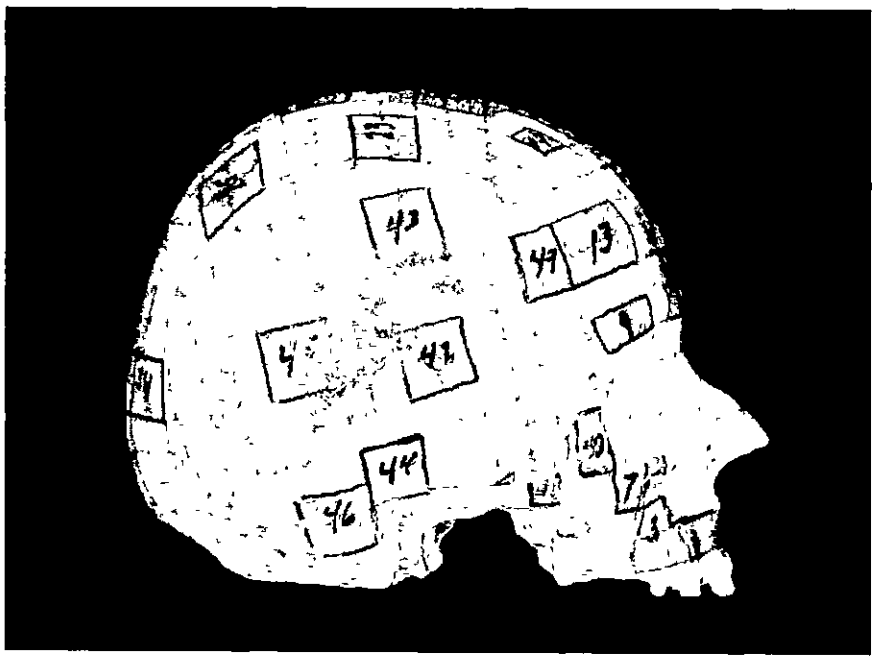


Figure 5. Right Norma Lateralis Gridding Scheme.

These samples were derived from the zygomatic, temporal, parietal and frontal bones (Table 3).

TABLE 3.--Visual Key for Right Norma Lateralis. Bone sample numbers (40-47).

Tooth/sample #	Symmetrical/Asymmetrical	Sample Location (Bone)
40,41,	Symmetrical	Zygomatic
42	Symmetrical	Temporal/Parietal
44,46	Symmetrical	Temporal
43,45	Symmetrical	Parietal
47	Symmetrical	Frontal

The eight samples selected on the left norma lateralis view were an approximate mirror image of the those selected from the right side of the skull (Figure 6).

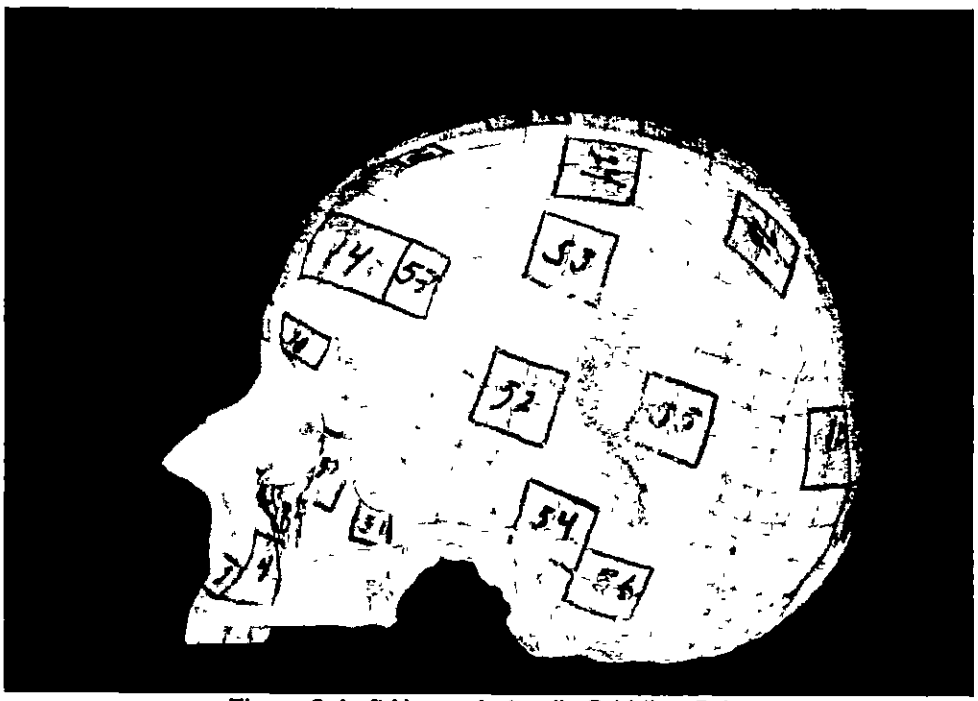


Figure 6. Left Norma Lateralis Gridding Scheme

TABLE 4.—Visual Key for Left Norma Lateralis. Bone sample numbers (50-57).

Tooth/sample #	Symmetrical/Asymmetrical	Sample Location (Bone)
50,51	Symmetrical	Zygomatic
52	Symmetrical	Temporal/Parietal
54,56	Symmetrical	Temporal
53,55	Symmetrical	Parietal
57	Symmetrical	Frontal

Sampling from the superior portion of the cranial vault was comprised of seven bone pieces (Figure 7).

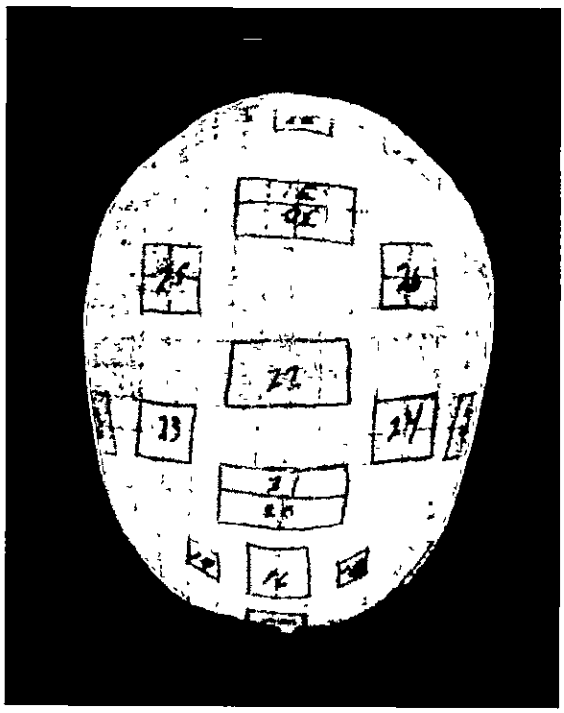


Figure 7. Norma Superioris Gridding Scheme.

The samples, which represented the norma superioris view, were acquired from the frontal and parietal bones (Table 5).

TABLE 5.--Visual Key for Norma Superioris. Bone sample numbers (20-26).

Tooth/sample #	Symmetrical/Asymmetrical	Sample Location (Bone)
20,21	Asymmetrical	Frontal
22	Asymmetrical	Parietal
23,24,25,26	Symmetrical	Parietal

Eight sample sites were selected from the cranial base (Figure 8).

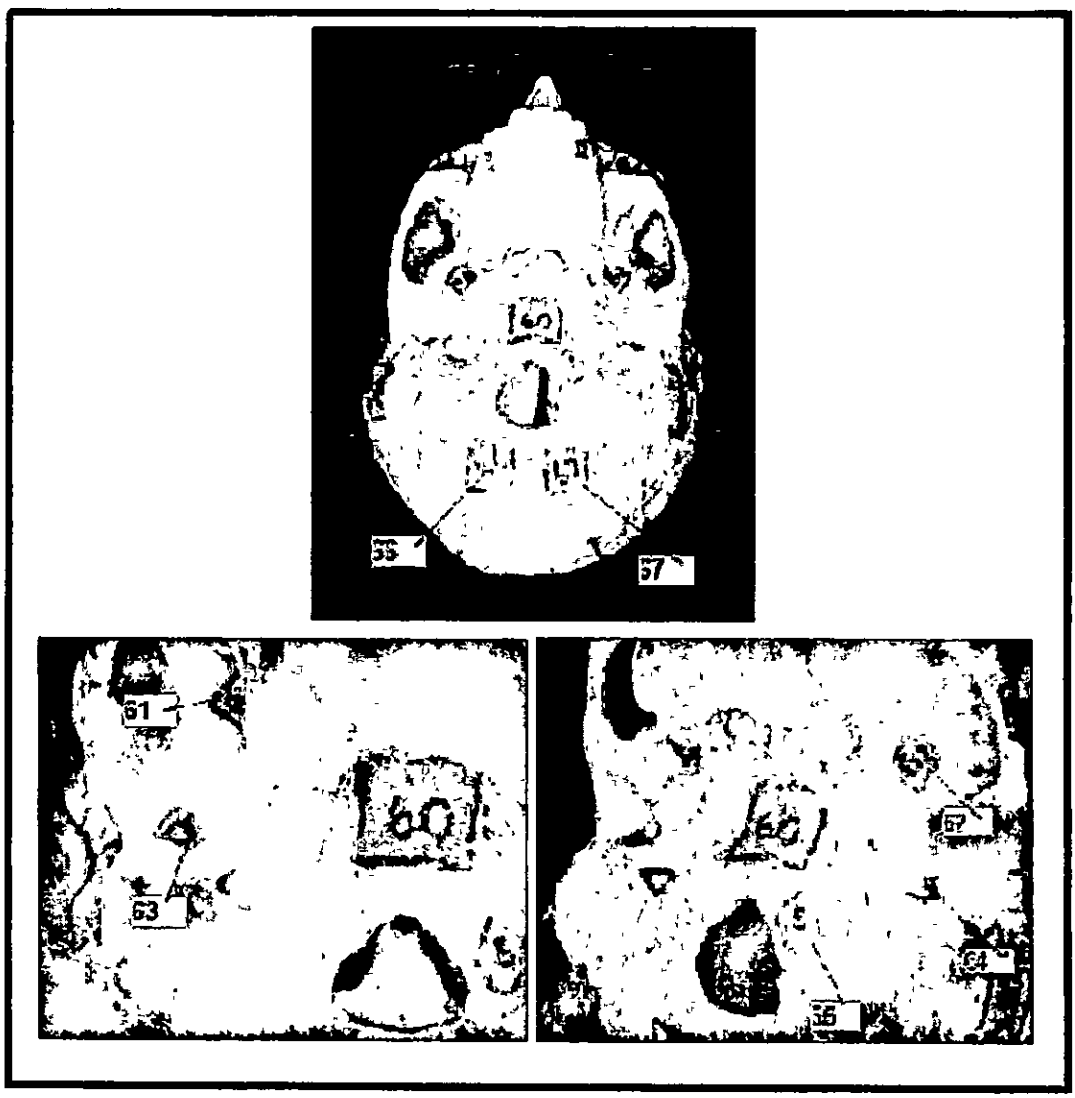


Figure 8. Norma Basalis Gridding Scheme.

The samples which comprise this view were derived from the occipital and sphenoid bones (Table 6).

TABLE 6.–Visual Key for Norma Basalis. Bone sample numbers (60-65).

Tooth/sample #	Symmetrical/Asymmetrical	Sample Location (Bone)
60	Assymetrical	Occipital
61, 62	Symmetrical	Sphenoid
63,64	Symmetrical	Temporal
65	Assymetrical	Occipital (Condyle)
66,67	Symmetrical	Occipital

By using the symphysis as a midpoint, the mandible was divided into right and left mirror images with each half comprising eight sections. In addition, three mandibular teeth (one incisor, one canine, and one premolar) were selected for testing (Figures 9, 10).

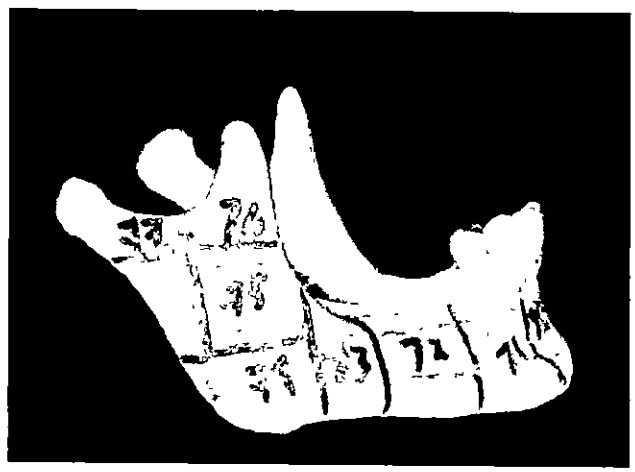


Figure 9. Right Mandibular Gridding Scheme.

Sampling of the mandible included the body, coronoid process, condylar process and alveolar process (Tables 7, 8).

TABLE 7.—Visual Key for Right Mandibular Bone and Teeth. Bone and tooth sample numbers (70-77 and mandibular teeth).

Tooth/sample #	Symmetrical/Asymmetrical	Sample Location (Bone)
70,71,72,73,74,75	Symmetrical	Mandible
76	Symmetrical	Mandible (Coronoid Process)
77	Symmetrical	Mandible (Condylar Process)
*mani ,*manc, *manp	Asymmetrical	Mandible (Alveolar Process)

*mani - mandibular incisor, *manc – mandibular canine, *manp – mandibular premolar

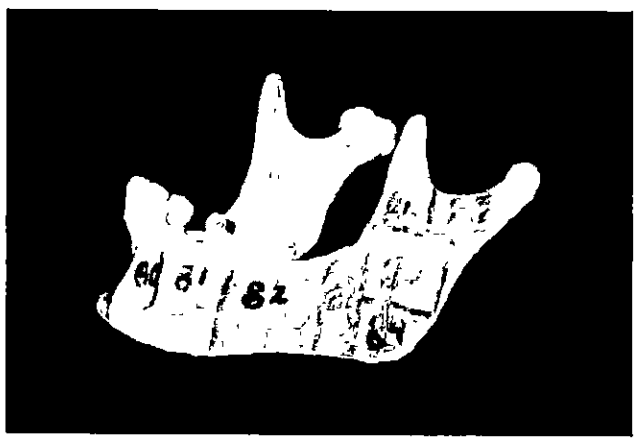


Figure 10. Left Mandibular Gridding Scheme.

TABLE 8.—Visual Key for Left Mandibular Bone. Bone sample numbers (80-87).

Tooth/sample #	Symmetrical/Asymmetrical	Sample Location (Bone)
80,81,82,83,84,85	Symmetrical	Mandible (Body)
* 86	Broken	Broken
87	Symmetrical	Mandible (Condylar Process)

* Bone piece 86 shattered during processing in the bone micro-machining device (Fig. 11).

Samples were sectioned using a Dremel™ (Racine, Wisconsin) drill mounted with a sectioning disk (Fig. 11b).

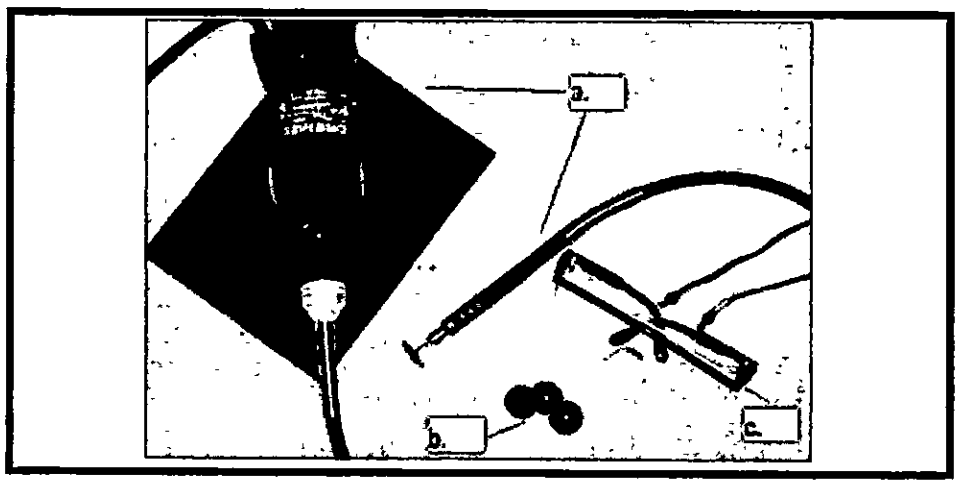


Figure 11. Instruments Used in Skull Sectioning. (a) Dremel™ electric motor and hand-piece, (b) sectioning disks, and (c) safety glasses.

Sectioning occurred while the bone was frozen (unthawed) and moistened with 7 pH distilled water. To prevent possible infection, I wore a mask, gloves, and a gown, and prepared bone specimens under a ventilation hood. Upon removal from the skull, each bone sample was immediately wrapped in muslin which had been soaked in distilled 7 pH water. Each sample was then placed in its own airtight plastic freezer bag and frozen at -4°C.

Micromachining was done on a Denham (Denford, Yorkshire, UK) Micromill™ 2000 CNC (Computer Numerical Control) saw. This device takes rough, manually cut

specimens and produces a flat surface with 0.1 mm accuracy (Figure 12).

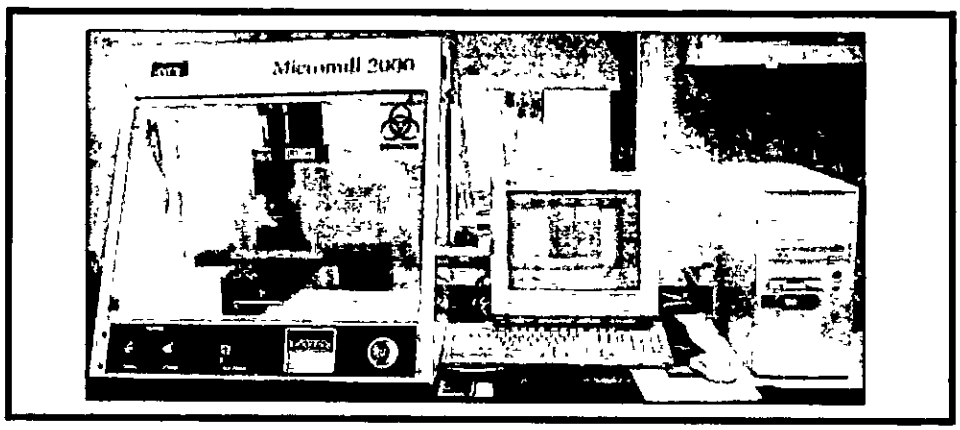


Figure 12. Bone Micro- Machining device. Denham (Denford, Inc.) Micromill 2000 CNC used to produce a flat surface on the cortical bone.

The milling of the external surface insures that a flat, cortical bone surface will be found orthogonal to the sound wave emitted by the scanning acoustic microscope (SAM) transducer and the tetrahedral Microindenter head. Finally, the external surfaces of the resulting pieces are manually fine polished using alumina gel and water. I began with 5 μm grit and worked my way through 1 μm, 0.33 μm to 0.15 μm fine grit.

4.3 Mass Density Recording

Water volume and wet weight was collected for each polished bone piece. Each specimen was pre-wetted (i.e.,

submerged for 5 min) in distilled, pH-neutral, water. It was then weighed to the nearest 0.1 mg using an OHAS (Pine Brook, NJ) Adventurer™ electronic scale. The sample was then transferred to a KIMAX™ (Vineland, NJ) 25 ml graduated cylinder where the volume of water displacement was measured to the nearest 0.1 ml. The readings for both weight and volume were taken 3 times (Table 10). These data were collected to produce a mass density baseline for removal of partial volume error from the radiodensity (intensity) data obtained later obtained from a CT-scan of the same bone pieces.

4.4 Scanning Acoustic Microscopy

An Olympus (Tokyo, Japan) UH3™ Scanning Acoustic Microscope (SAM) was used to measure sound impedance (Figure 13).



Figure 13. Scanning Acoustic Microscope (SAM). Olympus, Inc. SAM measures sound impedance.

Impedance is a surrogate measure for cortical bone stiffness. Impedance was recorded on the SAM in volts resistance. The SAM has a burst mode (i.e., perpendicular to the surface) and a pulse (i.e., parallel to the surface) mode. The burst mode was employed to measure impedance at the external surface of the prepared cortical bone pieces. A 400 Mhz burst mode lens was used to focus on a 0.5 mm spot. The specimen and a control phantom, a flat piece of steel, were mounted and leveled in a dish (Figure 14).

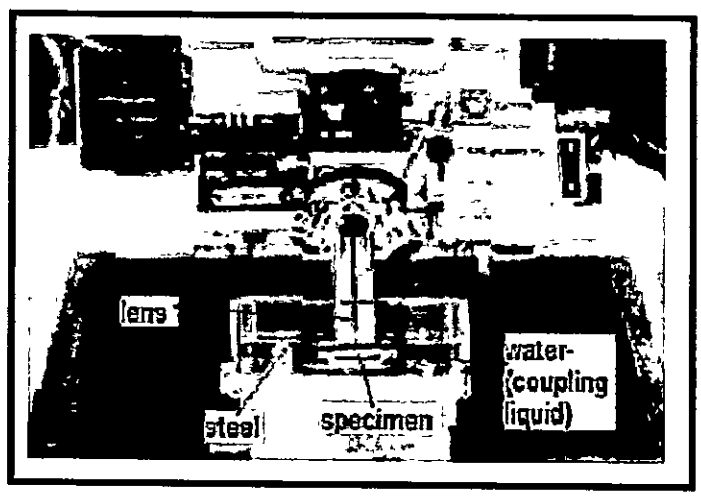


Figure 14. SAM Specimen Mounting. Specimen mounted and leveled in petri dish.

Distilled water acted as a coupling liquid between the SAM lens and the sample to be measured after it had been

placed in the dish. The water acted to couple the bone specimen and steel to the SAM lens thereby facilitating sound wave conductance. Before and after the bone value was taken, the steel was read to calibrate any changes that may have occurred in the device output or sensor reading. The signal amplitude obtained is proportional to acoustic reflectivity. Acoustic reflectivity is a function of the acoustic impedance of the bone's material properties at the external surface corrected for the coupling liquid (Bumerraj and Katz 2001). After an initial spot reading, additional readings were taken 0.1 mm in both directions of x and y. A total of 5 readings were taken for each point on each piece of bone (Appendix, Table 11). These spots were identified with indelible marker (Figure 15).

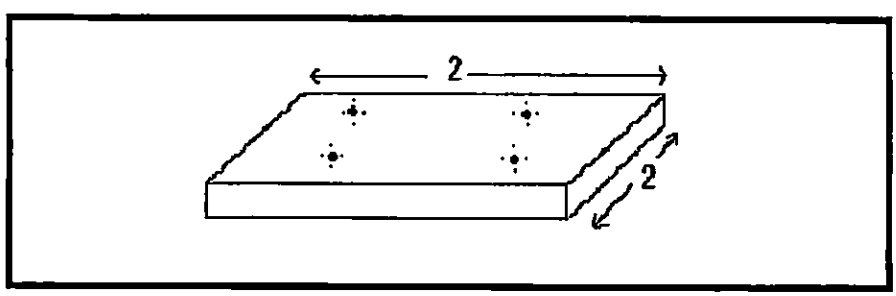


Figure 15. Sampling Pattern for the Scanning Acoustic Microscope (SAM). An example of a 2 x 2 cm bone sample (1 testing point for each 1 x 1 cm segment) with 4 additional readings around each point.

4.5 Microindentation

The process of microindentation began with the placement of each bone sample into a mount made of Triad™ acrylic (Densply, York, PA). The base allowed leveling and affixing of the specimen to prevent sliding and tipping during the measurement process. Building of the base was accomplished by placing the Triad™ material on a clear sheet of Endure™ retainer material (Great Lakes Orthodontics®, Tonawanda, NY). The bone to be sampled was placed in the Triad™ acrylic and leveled using a glass coverslip and bubble level (Figure 16).

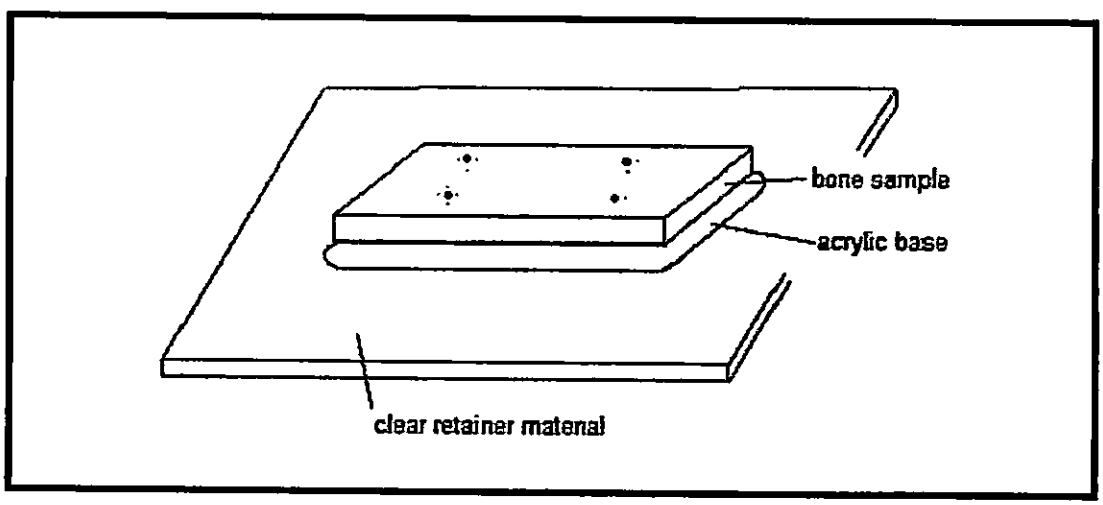


Figure 16. Mounting of Bone Sample on Acrylic Base.

The bone sample with the Triad acrylic base was set using a Unitek™ Ortholux™ XT curing light (3M, St. Paul, MN) for 40 seconds on each side (Figure 17).

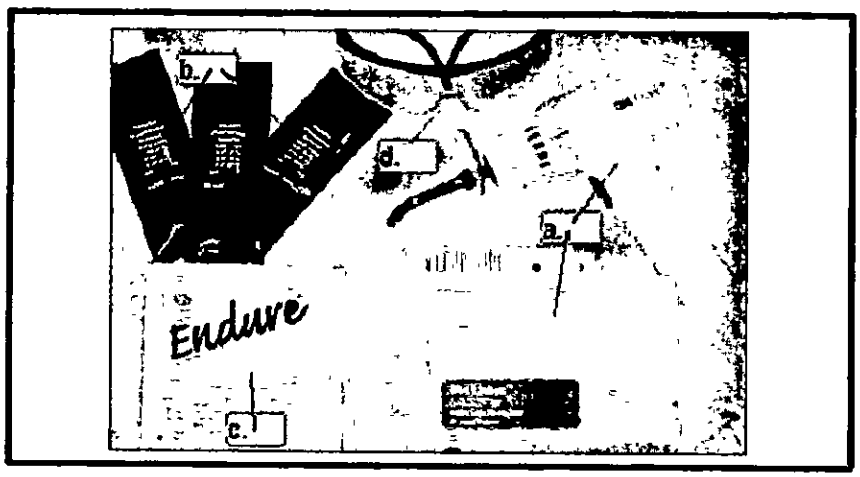


Figure 17. Instruments and Materials for Basing of Specimen for Microindentation. (a.) Ortholux™ XT curing light, (b.) Triad™ acrylic, (c) Endure™ invisible retainer material were used in the fabrication of microindentation mounting bases for each bone piece.

The sample was now ready for microindentation testing. The spots measured by microindentation were those marked with indelible marker prior to taking readings with the SAM. A Buehler™ microindenter (Buehler Inc., Lake Bluff, IL) was used to measure resistance to fracture, a surrogate measure for strength, with a "Vicker's" test (Huja et al. 1998) (Figure 18).

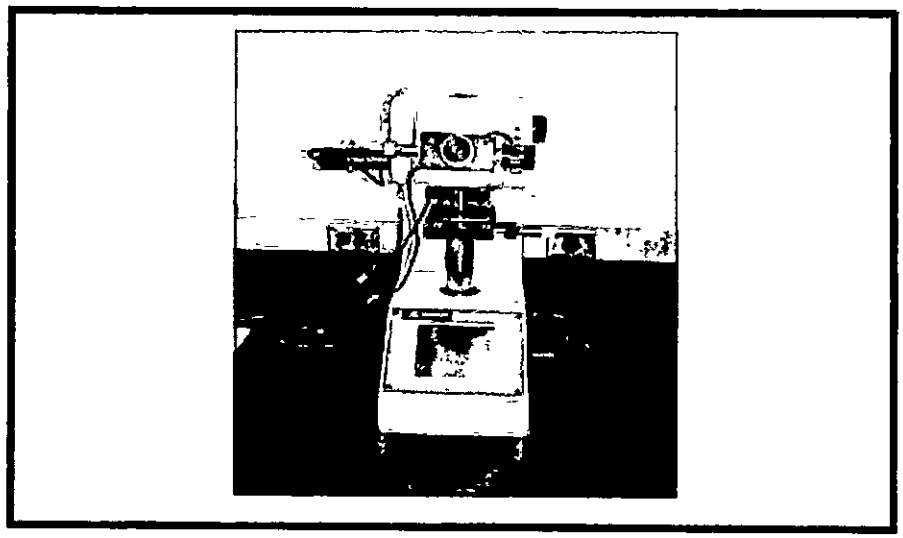


Figure 18. Microindenter. Buehler Inc. micro-indenter measures strength.

The indenter head has a known maximum impression diameter, (d) and is applied at a known load, (L). The diamond-tipped head forms a 5-10 μ tetrahedral impression following application of a 25-500 g load (Figure 19).

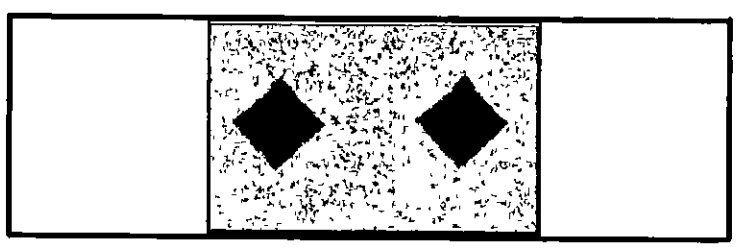


Figure 19. Diamond-head Impressions from Microindenter.

A load of 50 g was used in this study. The further the diamond-head enters the material, the wider the resulting impression. If the surface is orthogonal the width of the impression will equal the height. If indentation is too deep it will be round, not diamond shaped. All indentation readings were made at 200X through an eyepiece micrometer and were visualized with reflected light. The adjustable micrometer in the eyepiece was orientated so that "diameter" readings were made along the horizontal width of the indentation. The resulting Vicker's value, H_v(i.e., Vicker's hardness), is 1.854 times force (measured in kilograms) divided by the square of the impression diameter (measured in millimeters)(Klein 1989). After the initial spot reading, additional readings were taken 0.1 mm a part in both directions of x and y. Three readings were taken at each point (Appendix, Table 12).

4.6 Isolated Piece CT Scanning

CT-scanning of the isolated bone pieces and teeth was accomplished using a Philips Multislice™ CT scanner (Eindhoven, Netherlands) located at University Hospitals in Cleveland, Ohio. In order to separate the bone pieces from the scanning bed, a 3 inch layer of packing foam was

initially placed on the bed followed by a bed sheet. On top of the sheet the bone pieces with the bases were set in a linear fashion with 1 cm separation between pieces. A typical scan series would usually contain 3000 slices and 23-32 pieces of bone. Each piece of bone contained its own individualized slice sequence which ranged from 60 to 110 slices. At the completion of scanning a digital photograph was taken of the bone arrangement on the scanning bed to act as a map for segmenting the bone. The CT images were then transferred to my computer for segmentation.

4.7 Segmentation

Segmentation of the images was done on a Silicon Graphics™ R10K Octane computer (Mountain View, CA). The process of segmentation involved removing all visible artifacts from the image slices so that only the bone piece and air (i.e., 0 intensity) are left. Segmentation was accomplished with the use of a locally written program called AUTO (Dean et al. 1997). The purpose of this program is to allow the user to view image slices, and segment (retain) areas of interest. The user can select regions in multiple slices, mark the areas needed, and etch away unneeded areas. In the Image Options Menu,

I selected the RUB OUT tool in the Draw/Fill category and ROI in the Mouse Select category (Figure 20).

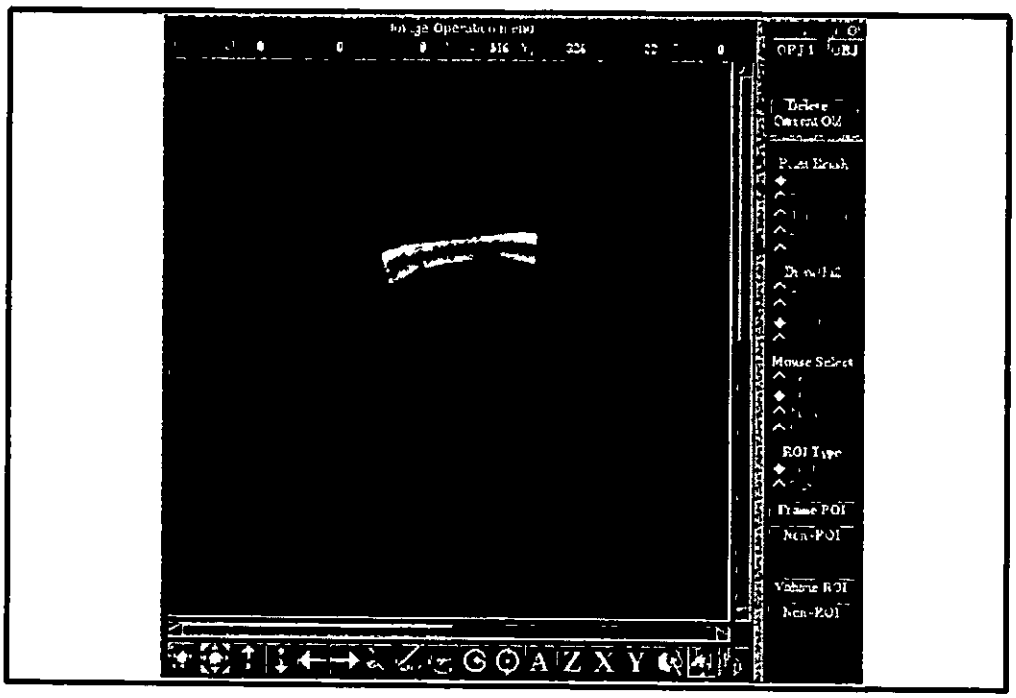


Figure 20. Bone Piece and Arcylic Base Pre-Segmentation. The segmentation process was accomplished using a locally derived program called AUTO.

Activation of RUB OUT and ROI allows removal of anything (any image) which is located within the region of interest (ROI). Once each slice had undergone segmentation the WRITE option was used to save the modified image. When the entire image sequence had undergone segmentation it was saved to a new directory.

The slices for each bone piece or tooth were segmented in this fashion and saved to a new directory (Figure 21).

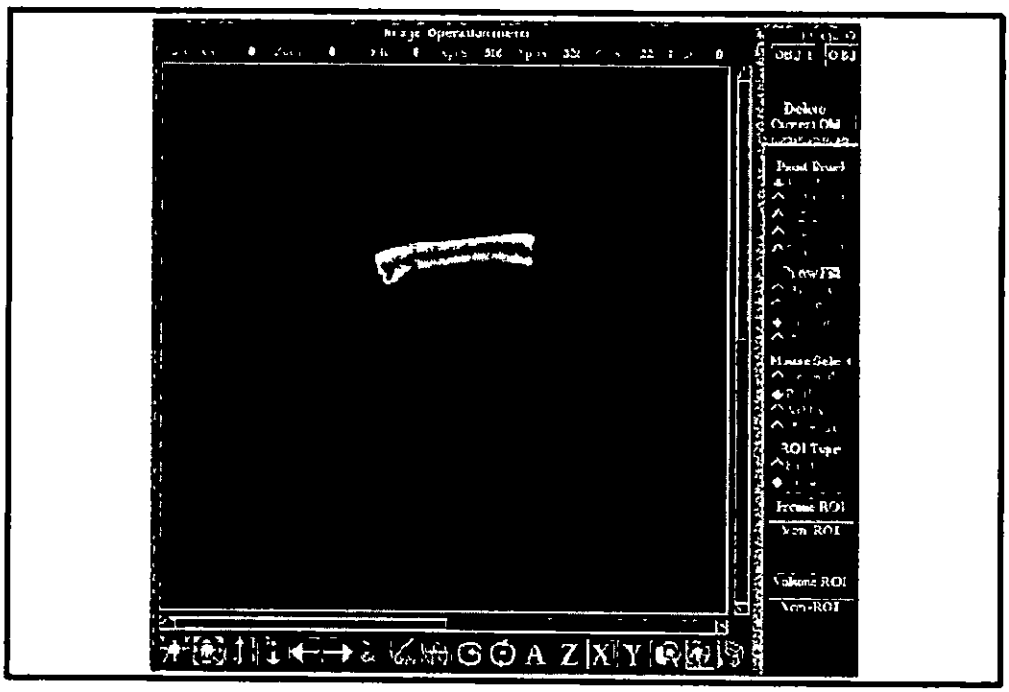


Figure 21. Bone Piece Post Segmentation. Everything in the slice image has been removed except for the bone in order to get accurate radiointensity readings.

Next, the average and standard deviation of intensity value of only the cortical bone portion could be calculated without the presence of air or trabecular bone (Dean et al. in press). This process is called partial volume error correction and is based on the pixels which comprise the image. The pixel intensity values are based on the Hounsfield scale with 0 being absolute black

(i.e., air) and 4096 being absolute white (i.e., most dense). Partial volume correction automatically eliminates any pixel with a Hounsfield intensity of 50 or less. The next step is to evaluate the maximum intensity range, usually between 1500-3500 Hounsfields for human cortical bone and teeth, and eliminate the trabecular bone pixels up to approximately 1500 Hounsfield. The average and standard deviation radiointensity (Hounsfields) would be based on the cortical bone intensity range alone (Dean *et al.* in press).

4.8 Statistical Analysis

All measurements were entered into a Microsoft™ Excel© spreadsheet for compilation and statistical analysis. For each bone and tooth sample, the average and standard deviation were recorded for mass-density, scanning acoustic microscope voltage, Vicker's hardness, and radiodensity (Table 9). The testing, which generated these averages and standard deviations, was specific for each material property.

The raw data for mass-density (Table 10) was based on three volume displacement measurements and three mass measurements. For each trial the mass was divided by the volume for mass-density measurements. The average and

standard deviation for each piece was based upon three trials.

The raw data for scanning acoustic microscope voltage (Table 11) was based upon the number of points which comprise the sample piece. Each 1 x 1 cm section of the sample was a point. Voltage data was collected from the point and four additional sites for a total of five readings per point. Point averages and standard deviations were made based on the five readings. The voltage average and standard deviation for each piece was based on the point averages.

The raw data collected from the microindenter (Table 12) was based on the same 1 x 1 cm sample points used in the scanning acoustic microscope. However, the impression data was collected from the point and two additional sites for a total of three readings. The Vicker's hardness value average and standard deviation was based on the point averages.

5. RESULTS

5.1 Summary Data Table

The Summary Table Data (Table 9) includes average and standard deviations for mass-density, SAM voltage, and Vicker's hardness, and radiodensity values for the seventy-seven bone pieces and six teeth which sampled the craniofacial complex of a 75-year-old female fresh-frozen cadaver. Non-destructive determination of these material properties was accomplished using mass-volume and radiodensity (via 3D CT) readings (density), scanning acoustic microscopy (stiffness), and microindentation (strength).

The mass and volume of each sample was recorded three times to the nearest tenth (grams for mass and milliliters for volume). From these values, mass density was calculated by dividing mass volume. Averages and standard deviation for each sample's mass-density appear in Table 9. These values were used for correction of partial volume error in determining radiodensity (Dean et al. in press.).

The scanning acoustic microscope readings for each piece started and finished with a stainless steel reading that acts as a calibration for the SAM electronics. Once the value for steel had been recorded, each 1 x 1 cm region of the sample would be sampled at least five times. All readings for the piece were then treated as a whole. The piece average and standard deviation values are reported in the Summary Data Table (Table 9).

The strength at the same positions where SAM readings were taken was represented by a microindenter recording. These values were converted to the Vicker's hardness scale. Each reading was repeated three times. As with the SAM data, the readings at the five points on each piece are presented as a single piece average and standard deviation in the Summary Data Table (Table 9).

Radiodensity values are derived from the partial-volume corrected segmentation data. Radiodensity is reported as the average intensity of cortical bone where the gray scale is 0, (absolute black or air) to 4096 (absolute white or most dense). Each piece was segmented from all other objects in the CT-scan. The average and standard deviation of the resulting cortical bone

radiodensity values is reported in Summary Data Table (Table 9).

The Summary Data Table (Table 9) allows me to determine radiodensity and the material properties of stiffness and strength.

TABLE 9.--Summary Data Table. Data Summary for the Material Properties of Density, Stiffness, and Strength for the Craniofacial Complex of a Fresh-Frozen Cadaver Bone.

Bone Piece #	Mass Ave (g/cm^3)	Mass STD	SAM Ave (Volts)	SAM STD	Pre Steel	Post Steel	Vicker's hardness value	Vik STD	Radio Ave (Hounsfields)	Radio STD
1	1.0	0.01	1.7	0.19	2.9	2.9	133.4	83.23	3075.04	443.15
1a	1.0	0.01	1.3	0.52	3.5	3.5	36.6	10.50	2077.54	316.69
2	2.1	0.00	1.1	0.57	2.8	2.8	106.3	3.30	3113.39	405.07
2a	1.7	0.00	1.1	0.50	2.8	2.8	39.3	23.93	2164.56	244.14
3	1.5	0.00	0.9	0.00	2.4	2.4	144.1	54.30	2515.05	168.88
3a	1.4	0.00	0.8	0.05	2.4	2.4	126.3	41.72	2396.78	260.40
4	1.5	0.00	0.7	0.25	1.9	1.9	127.9	1.24	2301.50	521.79
5	1.1	0.00	0.5	0.05	1.6	1.6	133.8	15.82	2064.31	369.87
6	1.5	0.00	0.8	0.17	1.6	1.6	239.1	75.20	2277.59	241.19
7	2.4	0.00	0.7	0.13	2.4	2.4	89.5	81.41	2593.71	252.20
8	1.4	0.00	1.4	0.02	2.1	2.1	74.4	68.19	2352.11	281.27
9	1.6	0.00	1.4	0.02	2.3	2.3	132.5	15.77	2621.25	373.27
10	1.3	0.00	1.4	0.01	2.4	2.4	131.6	5.26	2336.66	444.87
11	1.4	0.00	1.5	0.27	2.9	2.9	88.9	23.77	2605.90	310.19
12	2.0	0.00	1.8	0.00	2.9	2.9	132.5	58.50	2816.88	260.08
13	1.5	0.06	2.2	0.81	1.9	1.9	65.7	15.93	2726.66	304.49
14	1.4	0.00	1.6	0.12	1.9	1.9	80.3	58.34	2550.26	384.88
15	1.8	0.00	1.0	0.59	2.0	2.0	101.5	82.48	2844.84	240.34
16	2.0	0.08	1.8	0.18	2.0	2.0	60.1	27.52	2932.35	270.95
17	1.8	0.00	1.5	0.08	2.0	2.0	111.2	43.33	2914.85	284.37

TABLE 9.–Summary Data Table. Data Summary for the Material Properties of Density, Stiffness, and Strength for the Craniofacial Complex of a Fresh-Frozen Cadaver Bone (continued).

Bone Piece #	Mass Ave (g/cm^3)	Mass STD	SAM Ave (Volts)	SAM STD	Pre Steel	Post Steel	Vicker's hardness value	Vik STD	Radio Ave (Hounsfields)	Radio STD
18	1.3	0.00	1.7	0.18	2.5	2.5	140.9	85.58	2629.72	266.55
20	1.6	0.08	2.0	0.15	2.7	2.7	31.3	2.18	2840.57	254.47
20a	1.5	0.10	2.1	0.16	2.7	2.7	19.0	13.62	2827.59	296.11
21	1.8	0.00	2.0	0.11	2.6	2.6	7.4	0.11	2860.18	243.87
21a	1.8	0.00	2.0	0.09	2.6	2.6	15.2	1.93	2865.37	259.72
22	1.4	0.12	1.9	0.24	2.5	2.5	28.1	6.19	2826.01	260.12
22a	1.9	0.10	1.8	0.21	2.5	2.5	27.7	9.45	2838.47	260.91
23	1.6	0.00	1.6	0.10	2.5	2.5	26.8	11.09	2819.37	306.47
24	1.4	0.00	1.7	0.21	2.5	2.5	20.8	11.66	2705.48	305.71
25	1.5	0.00	0.9	0.22	2.9	2.9	21.2	3.50	2827.61	251.93
26	1.5	0.00	1.8	0.16	2.9	2.9	26.3	5.72	2785.22	253.71
30	1.4	0.04	1.5	0.30	2.5	2.5	17.4	8.27	2809.17	261.14
31	1.7	0.04	1.4	0.51	2.5	2.5	26.1	7.71	2826.51	251.16
32	1.4	0.00	1.4	0.35	2.4	2.4	17.0	5.93	2766.44	348.37
33	1.6	0.00	1.9	0.22	2.4	2.4	17.8	5.09	2697.22	338.76
34	1.5	0.00	1.6	0.44	2.4	2.4	17.2	5.27	2817.29	269.15
35	1.6	0.00	1.6	0.30	2.4	2.4	17.8	4.14	2896.55	281.07
36	1.5	0.00	1.7	0.08	2.6	2.6	19.0	7.55	2889.28	270.58
40	1.2	0.00	1.8	0.40	2.5	2.5	52.4	4.07	2947.20	322.13
41	1.5	0.00	1.7	0.13	2.5	2.5	66.0	1.93	2410.37	311.66
42	1.3	0.04	1.8	0.08	2.5	2.5	49.5	20.74	2880.87	264.78
43	1.3	0.04	1.7	0.19	2.5	2.5	43.1	19.08	2355.63	480.72
44	1.8	0.00	2.0	0.11	2.5	2.5	27.8	8.21	2675.25	363.43
45	1.4	0.00	1.9	0.21	2.7	2.7	19.6	11.88	2597.69	332.85
46	1.4	0.00	1.9	0.13	2.7	2.7	25.7	4.86	2838.13	391.56
47	1.3	0.07	2.1	0.09	2.5	2.5	45.1	21.62	2358.73	362.14
50	1.2	0.00	2.0	0.08	2.5	2.5	62.2	9.09	3021.76	339.68

TABLE 9.–Summary Data Table. Data Summary for the Material Properties of Density, Stiffness, and Strength for the Craniofacial Complex of a Fresh-Frozen Cadaver Bone (continued).

Bone Piece #	Mass Ave (g/cm^3)	Mass STD	SAM Ave (Volts)	SAM STD	Pre Steel	Post Steel	Vicker's hardness value	Vik STD	Radio Ave (Hounsfields)	Radio STD
51	1.5	0.00	2.1	0.11	2.5	2.5	27.5	7.79	2381.94	350.30
52	1.6	0.00	2.1	0.06	2.7	2.7	117.3	28.93	2874.56	258.83
53	1.6	0.00	2.0	0.21	2.7	2.7	60.9	25.72	2663.24	342.95
54	1.6	0.00	2.1	0.12	2.7	2.7	86.6	14.99	2779.49	375.00
55	1.8	0.09	2.0	0.10	2.7	2.7	37.2	21.80	2748.01	281.16
56	1.7	0.06	1.9	0.19	2.7	2.7	35.0	20.84	2868.81	321.91
57	1.8	0.00	2.0	0.26	2.7	2.7	66.7	16.80	2698.56	280.59
60	1.6	0.00	1.6	0.14	2.5	2.5	16.5	1.47	1946.71	369.54
61	1.5	0.00	1.9	0.02	2.5	2.5	78.0	8.50	2623.89	184.86
62	1.4	0.24	2.1	0.02	2.5	2.5	66.4	17.77	2043.97	220.20
63	3.0	0.00	1.9	0.29	2.8	2.8	60.1	1.45	3006.35	310.81
64	2.5	0.00	2.0	0.05	2.8	2.8	70.4	6.34	2960.98	299.95
65	1.5	0.00	2.1	0.16	2.7	2.7	18.5	5.17	2224.69	461.23
66	1.5	0.16	1.8	0.16	2.7	2.7	16.9	9.67	2949.83	289.63
67	1.8	0.00	1.8	0.17	2.7	2.7	31.3	18.68	2915.07	281.36
70	1.6	0.00	1.6	0.08	2.3	2.3	72.8	11.78	2771.15	319.30
71	1.4	0.00	1.8	0.10	2.4	2.4	48.5	8.43	2889.68	370.55
72	1.4	0.00	1.5	0.26	2.4	2.4	51.2	13.81	2732.14	465.81
73	1.4	0.06	1.5	0.16	2.3	2.3	56.4	9.81	2845.38	389.30
74	1.6	0.00	1.4	0.26	2.9	2.9	19.7	4.68	2908.52	346.24
75	1.4	0.00	1.7	0.10	2.9	2.9	25.7	13.09	2565.34	570.90
76	1.8	0.00	1.3	0.19	2.9	2.9	42.2	16.78	2996.51	306.13
77	1.4	0.00	1.6	0.18	2.9	2.9	46.2	11.97	2797.57	393.45
80	1.4	0.00	1.4	0.23	2.9	2.9	62.8	25.32	2296.08	422.26
81	1.4	0.00	1.6	0.22	2.8	2.8	47.5	6.50	2690.54	543.40
82	1.2	0.00	1.4	0.17	2.8	2.8	74.5	27.62	2457.17	563.33
83	1.3	0.00	1.8	0.15	3.0	3.0	33.4	15.21	2642.75	518.72
84	1.3	0.00	1.8	0.16	3.0	3.0	19.2	13.14	2376.22	522.32
85	1.4	0.00	1.6	0.11	3.0	3.0	52.8	11.27	2469.04	617.50

TABLE 9.–Summary Data Table. Data Summary for the Material Properties of Density, Stiffness, and Strength for the Craniofacial Complex of a Fresh-Frozen Cadaver Bone (continued).

Bone Piece #	Mass Ave (g/cm^3)	Mass STD	SAM Ave (Volts)	SAM STD	Pre Steel	Post Steel	Vicker's hardness value	Vik STD	Radio Ave (Hounsfields)	Radio STD
87	1.6	0.00	1.7	0.14	2.8	2.8	59.6	18.12	3027.83	355.47
*mani	2.1	0.18	2.4	0.18	2.8	2.8	251.9	20.08	3247.27	340.44
*manc	2.2	0.00	2.6	0.01	2.8	2.8	199.1	44.40	3213.97	393.92
*manp	2.1	0.21	2.6	0.05	2.8	2.8	240.6	43.23	3104.73	609.10
*maxi	2.2	0.00	2.7	0.04	2.8	2.8	233.6	11.58	3299.28	325.91
*maxc	2.0	0.00	2.6	0.11	2.8	2.8	268.5	19.64	3249.51	317.91
*maxp	2.0	0.00	2.6	0.01	2.8	2.8	276.2	2.51	3066.07	577.79

*mani- mandibular incisor, *manc- mandibular canine, *manp- mandibular premolar
*maxi- maxillary incisor, *maxc- maxillary canine, *maxp- maxillary premolar

5.2 Correlation between Radiodensity and Stiffness

Plotting radiodensity versus the SAM voltage, which is a measurement of stiffness, for both the cranial bone and teeth reveals a highly positive correlation ($r = 0.47$). Although there are several clear outlier points, an outlier analysis did not improve the correlation significantly. The strong overall trend demonstrates radiodensity increasing with increasing stiffness.

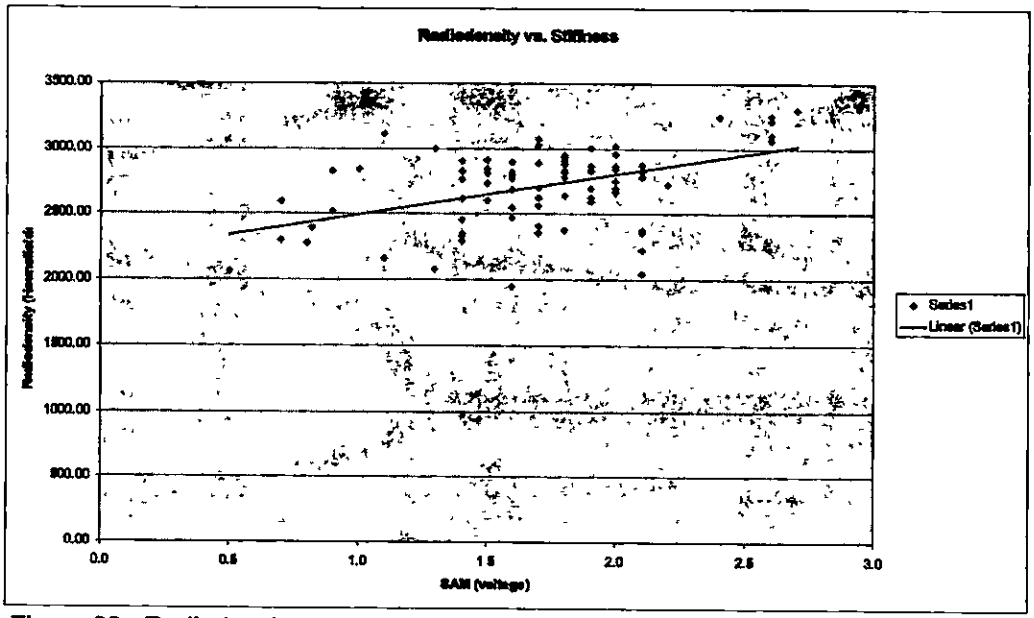


Figure 22. Radiodensity vs. Stiffness. Plotting of radiodensity versus stiffness for the the bone and tooth samples collected from the fresh-frozen cadaver (r = 0.47).

5.3 Correlation between Radiodensity and Strength

The relationship between radiodensity and strength, as measured by Vicker's hardness, showed a moderately positive correlation (r = 0.24). However, as with the stiffness, the correlation did not improve significantly with removal of outliers. Despite a greater spread of radiodensity values at each Vicker's hardness reading, the trend here was equally strong, showing a clear relationship between the increasing radiodensity and increasing strength.

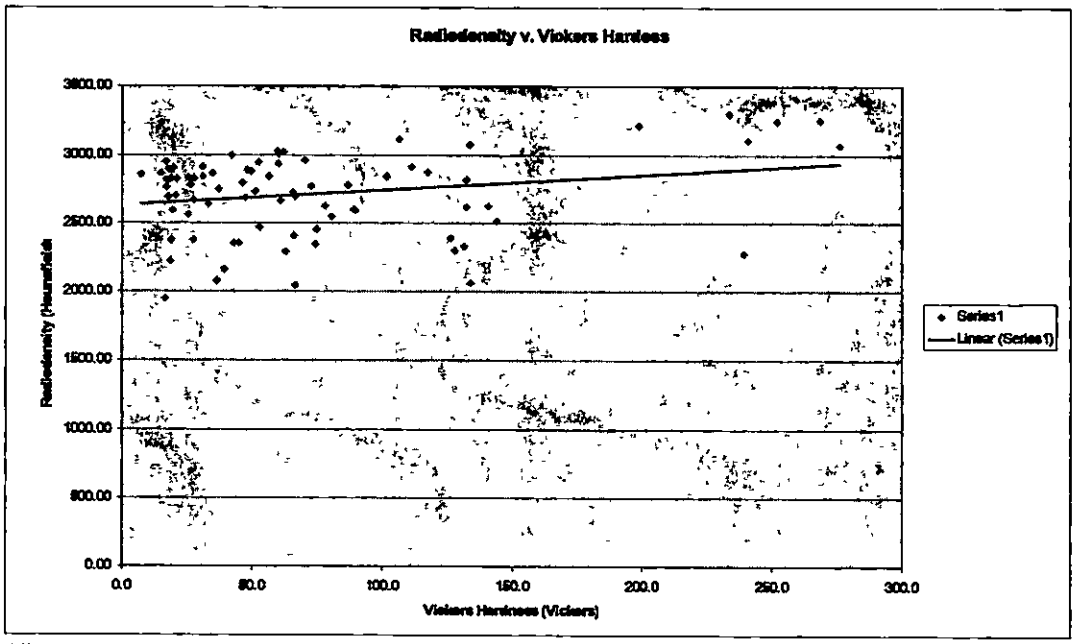


Figure 23. Radiodensity vs. Vicker's Hardness. Plotting of radiodensity versus Vicker's Hardness for bone and tooth samples collected from the fresh-frozen cadaver (r = 0.24).

6. DISCUSSION

6.1 Methodological Observations

The primary objective of this study was to determine if the material properties of the craniofacial complex of a 75 year old female fresh-frozen cadaver specimen were heterogeneous. One of the more challenging aspects of this endeavor was selecting the resolution at which to acquire the material property data, as this study attempted to sample the entire external surface of the craniofacial complex. This work was made easier by what was learned in a pilot study of the bovine cranium complex. The bovine study found a high degree of material property variation between regions of the cranium (Dean et al. in press.).

6.1.1 Specimen Acquisition and Gross Preparation

An important consideration in this study of the material properties is the age of the subject. Age is an important consideration since human bone tends to incur significant reductions in stiffness and strength with age (Zioupos and Currey 1998). Another consideration was how

the bone was maintained during storage and testing. During storage, preparation, and testing the samples were continually moistened with distilled pH 7 water and were wrapped and bagged to protect against freezer burn. The goal was to accomplish all measurements with the bone intact, especially its collagen, to mimic *in vivo* conditions, since drying or embalming of bone significantly changes the bone material properties, especially by affecting bone collagen composition (Zioupos and Currey 1998).

6.1.2 Fine Bone Preparation

Fine preparation of fresh-frozen bone was designed to create flat bone samples which would allow for the orthogonal head position required for the SAM and the microindenter. The CNC bone micro-machining device manually cut specimens to produce a flat surface with 0.1 mm accuracy. However, cortical plate thickness was sometimes insufficient; thus, the CNC would destroy the majority of the cortical layer in establishing a flat surface. In areas with a thin cortical plate use of a dental hand-piece with finishing burs to level the bone helped to retain an adequate cortical bone layer. In my opinion, the fine bone preparation was a critical step in

the study of the material properties, one where operator skill directly affected the quality of the data. Accurate and precise readings from both the SAM and microindenter were highly dependent on smooth, flat, and pit-less bone surfaces. A sample lacking any one of these qualities would likely result in unreliable material property readings.

6.1.3 Mass Density Measurements

Mass density was computed from volume measurements taken with a graduated cylinder with 0.2 ml measurement intervals for volume. Weight measurements were collected with an electronic scale. The limiting factor in the accuracy of the mass-density measurements was the volume reading. Accuracy to two tenths of a milliliter was made possible through the use of a graduated cylinder with a wide opening and small (i.e., 0.2 ml) interval marking. Another factor in measuring the mass density was the need to remove all the air from the bone sample in order to avoid air affecting the volume displacement or weight. The surface tension of water can lead to the entrapment of air. Therefore, I presoaked each bone piece. Visual inspection of the submerged bone sample was intended to prevent air bubbles from becoming trapped under the

sample. Possible enhancements to the volumetric readings could include switching the measuring medium to a noble gas, using a solution which has low surface tension and biocompatibility, or agitating the specimen during presoaking sufficiently to insure loss of entrapped air.

6.1.4 Scanning Acoustic Microscope

Initial use of the scanning acoustic microscope proved to be frustrating and unreliable. There was difficulty in focusing on the surface and the readings were unpredictable. The initial data collected was discarded due to the discovery of foreign debris clogging the lens. Once the lens was cleaned with an alcohol solution and rinsed with distilled water, the problems of focusing and reliability disappeared. Data acquisition with the scanning microscope required a smooth sample surface, as the acoustic impedance reading must reflect directly back from the sample. The SAM lens focuses on a 0.5 mm spot of cortical bone during burst mode. Any significant degree of surface imperfection scatters the reflected waves. Trabecular bone naturally possesses a great deal of porosity and cortical bone a moderate amount. However, the SAM focusing process allowed selection of a pit-free portion of the polished surface.

6.1.5 Microindentation

Microindention also depends heavily on the quality of bone surface preparation. Accurate readings require an adequate thickness of cortical bone to assure that the impression left by the indenter did not penetrated into the trabecular bone. In addition, a flat and smooth surface was also imperative so that the indenter's impression head would have an orthogonal approach to the bone or tooth specimen. Small surface imperfections could result in significant, but irreproducible readings.

6.1.6 Comparison of Sampling Techniques

Probably the most significant short coming of this study was the inability to choose a single resolution at which to sample all bone material properties. It would be ideal to have identical sampling volumes when determining density, stiffness, and strength. With the method used, bulk density was measured for the whole bone sample. However, microindentation was measured on the level of microns, and SAM samples a 0.5 mm "spot" area. Another important consideration is the ability to sample only the material properties of the cortical bone layer. The methods employed, SAM (stiffness) and microindentation (strength), measured the cortical bone

external surface, while mass density was being determined from the whole sample (i.e., both cortical and trabecular bone) and radiodensity was measured from isolated segmented cortical bone voxels. These measurements should ideally have been based on readings gathered from the same piece of isolated cortical bone. The resolution is also a question at the macro level as the location of bone "spots" or "pieces" sampled ideally must sample the entire range of bone structures present to give an accurate picture of the correlation between material properties (i.e., density, strength, stiffness, and geometry) of the entire craniofacial complex.

6.1.7 Segmentation

The initial process of segmentation was attempted using poor pixel resolution (i.e., pixel size of 0.X mm and slice thickness of 1.0 mm) in order to reduce the CT scanning time of the bone/tooth samples. This first pass CT-scanning was accomplished by placing 12-15 bone pieces in row with little, or no, room between rows. However, when calculations were completed for radiodensity, it was found that the standard deviation on some pieces nearly approached 100% of the average cortical bone value. The resolution was so low that the

partial volume error could not be adequately corrected and the data was useless. Rescanning the pieces with increased resolution, one at a time, zoomed all the way in, and allowed 10-20 times higher resolution per piece (i.e., pixel size 0.X mm, slice thickness 1.0 mm). After segmentation, the new calculations revealed radiodensity standard deviations near 10% and provided more reliable data.

6.2 Summary of Materials and Methods

In my opinion, the methods used to nondestructively obtain the stiffness (SAM) and strength (microindention) of bone may be too "micro" in relationship to the density measurements. These techniques are designed to obtain the material properties of various homogeneous artificially manufactured compounds which possess minimal porosity or surface roughness. The imperfections and porosities associated with bone make reliable data collection challenging.

6.3 Regional Results

One of the objectives of this study was to determine if the material properties (density, stiffness, and strength) of the craniofacial skeleton and teeth were homogeneous. The following is an evaluation of the range

of material properties obtained from each of the six skull views.

6.3.1 Material Property Ranges of Norma Frontalis

The ranges of the material properties of bone samples #1-18 (Table 9), gathered from norma frontalis (Figure 3) were:

Mass Density: (1.0 - 2.4) g/cm^3

SAM (Stiffness): (0.5 - 2.2) volts

Vicker's Hardness: (36.6 - 239.1)

Samples in this view showed a large degree of material property variance for density, stiffness, and hardness. The bone samples with higher density readings seemed to be located around the orbital rims; stiffness was generally higher across the frontal bone, and strength was greatest around the piriform rim and the superior portion of the frontal bone. The low mass density readings of 1.0 g/cm^3 were associated with bone pieces 1 and 1a. These samples were very small and thin and there was difficulty in recording the volume. The limitation of measuring to the nearest two tenths milliliter probably affected accuracy of the actual volume acquired. Another data outlier was associated with bone sample #6 and its Vicker's hardness value of 239.1 (Table 9). Two

of the three points measured on this piece had unusually high readings which caused an increase in the piece's average Vicker's hardness.

6.3.2 Material Property Ranges of Norma Superioris

The ranges of the material properties of bone samples #20-26 (Table 9), seen in norma superioris (Figure 7)were:

Mass Density: (1.4 - 1.9) g/cm^3

SAM (Stiffness): (0.9 - 2.1) volts

Vicker's Hardness: (7.4 - 31.3)

The highest bone density and stiffness readings were located in the anterior portion of the frontal and decreased slightly posteriorly in the parietals. The low SAM voltage value of 0.9 was associated with bone piece #25. Almost all the point value averages were extraordinarily low, so it is possible that the piece was not properly leveled or the machine was not properly focused, either of which would have caused lower readings. The bone sample #26, which is complementary (same relative location on left), displayed similar material properties except for SAM voltage (1.8).

6.3.3 Material Property Ranges of Norma Occipitalis

The ranges of the material properties of bone samples #30-36 (Table 9), seen in norma occipitalis (Figure 4):

Mass Density: (1.4 - 1.7) g/cm^3

SAM (Stiffness): (1.4 - 1.9) volts

Vicker's Hardness: (17.2 - 26.1)

Samples #30-36, gathered from the occipital region, displayed the least amount of bone material property variation compared to other regions sampled. Compared to the other regional material property ranges, the Vicker's hardness values were in a smaller range, which makes this region seem more homogeneous.

6.3.4 Material Property Ranges of Right Norma Lateralis

The ranges of the material properties of bone samples #40-47 (Table 9), seen in right norma lateralis (Figure 5) were:

Mass Density: (1.2 - 1.8) g/cm^3

SAM (Stiffness): (1.7 - 2.1) volts

Vicker's Hardness: (19.6 - 66) volts

A moderate degree of material property variation was displayed amongst samples #40-47. The highest degree of variation was at the interface between the zygomatic arch

and the temporal bone (sample #44). There was an increase in both mass density and strength of the zygomatic portion of the temporal bone relative to others in the region. The contralateral sample, #54, had similar material properties except for the Vicker's Hardness which was significantly greater.

6.3.5 Material Property Ranges of Left Norma Lateralis

The ranges of the material properties of bone samples #50-57 (Table 9), seen in left norma lateralis (Figure 6) were:

Mass Density: (1.2 - 1.8) g/cm^3

SAM (Stiffness): (1.9 - 2.1) volts

Vicker's Hardness: (27.5 - 117.3)

Samples #50-57, left norma lateralis, displayed a moderate degree of variation and the material properties were similar to those obtained from the right norma lateralis. The distribution of high and lower values between left and right norma lateralis were quite similar with the exception of an apparent Vicker's outlier. A Vicker's outlier value of 117.3 was seen in bone piece #52. There were unusually high Vicker's point averages on two of the four points, thus, raising the piece average. Without this outlier, the Vicker's hardness

range would have been from 27.5-86.6, thus making the Vicker's hardness ranges of the right and left norma lateralis nearly the same.

6.3.6 Material Property Ranges of Norma Basalis

The ranges of the material properties of bone samples #60-67 (see data in Table 9), seen in normal basalis (see key in Fig.8) were:

Mass Density: (1.4 - 3.0) g/cm^3

SAM (Stiffness): (1.6 - 2.1) volts

Vicker's Hardness: (16.5 - 78.0)

When evaluating bone pieces #60-67 there was again variation between the material properties. Bone samples #63 and #64, from the temporal bone (glenoid fossa), displayed increased mass density and stiffness when compared to the other regional samples. Right and left side comparisons revealed similar material property results. The upper mass density range of 3.0 g/cm^3 was obtained by an outlier piece, #63. Without this piece the mass density range would have been 1.4-2.5 g/cm^3.

6.3.7 Material Property Ranges of Right Mandible

The ranges of the material properties of these bone samples #70-77 (Table 9), seen in right mandibular view (Figure 9) were:

Mass Density: (1.4 - 1.8) g/cm^3

SAM (Stiffness): (1.3 - 1.8) volts

Vicker's Hardness: (19.7 - 72.8)

Mandibular bone samples #70-77 showed variance anteriorly-posteriorly. The mass density range was similar to that found in a study by Dabney and Dechow (2003). Material property ranges of mass density, stiffness, and strength, displayed a high-lower-high pattern. In the anterior portion of the mandible material properties were in the higher portion of their range. The body of the mandible displayed low to moderate material property range values which was then proceeded to increase posteriorly in the area of the ramus.

6.3.8 Material Property Ranges of Left Mandible

The ranges of the material properties of bone samples #80-87 (Table 9), seen in left mandibular view (Figure 10) were:

Mass Density: (1.2 - 1.6) g/cm^3

SAM (Stiffness): (1.4 - 1.8) volts

Vicker's Hardness: (19.2 - 74.5)

The material properties ranges of the left mandibular view were similar to those found on the right side. There was also moderate variation amongst the bone

samples anteriorly-posteriorly (a high-low-high gradient pattern) very similar to those described for the right mandibular view.

6.3.9 Material Property Ranges of Teeth

The ranges of the material properties of the three mandibular teeth and three maxillary teeth (Table 9), seen in left and right views (see keys in Figures 3, 9, and 10) were:

Mass Density: (2.0 - 2.2) g/cm^3

SAM (Stiffness): (2.4 - 2.7) volts

Vicker's Hardness: (199.1 - 276.2)

The variance in the material properties of the teeth was significantly less than the bone samples. Overall, the teeth overall displayed the highest density, stiffness and hardness values of nearly all the samples tested.

6.4 Summary of the Material Properties

Overall, the material properties of the bone sampled from the craniofacial complex showed considerable variation. Thus, a positive answer to the hypothesis, of H_o #1 (Chapter 3). However, this cannot be said for H_o #2. This might be due to the differences between the materials sampled for mass and radiodensity (i.e., whole bone piece in the former, only cortical bone voxels in

the latter), or due to the mismatch between whole piece bulk density versus SAM and microindentation spot size. Correlation between radiodensity and hardness, SAM, and modulus ranged between 0.2 and 0.4. However, another possibility for lack of a stronger correlation could be due to other factors, perhaps bone matrix geometry (Gibson 1997) or calcium phosphate crystal properties (Akkus 2003). If this were the case, improved density, SAM, and microindentation measurement accuracy alone would not improve the correlation between the bone material properties studied and radiodensity.

7. CONCLUSIONS

The purpose of this study was to determine whether radiodensity data obtained by CT-scan could be used to accurately predict the material properties of a patient's skull. If radiodensity is sufficiently correlated with stiffness and strength, it could be used to predict a craniofacial finite element model capable of simulating a patient's response to surgical or appliance treatment including the possibility of skeletal failure. The data showed that the material properties, stiffness and strength, varied across the specimen's craniofacial complex. Positive correlations were found between radiodensity and stiffness ($r = 0.47$) and radiodensity and strength ($r = 0.24$). However, it is important to remember that the results obtained from this study represent data from only one specimen. Continued studies on additional specimens would hopefully lend further validation to the results which were achieved from this project.

APPENDIX

TABLE 10.--Raw Data for Mass Density of Bone Pieces and Teeth.

Bone #	Weight	Volume	Density	Ave Density	Std Dev
Units	grams	ml	g/cm^3	g/ cm^3	
1	.104g	.1ml	1.04	1.0	0.01
	.103g	.1ml	1.03		
	.102g	.1ml	1.02		
1a	.104g	.1ml	1.04	1.0	0.01
	.103g	.1ml	1.03		
	.102g	.1ml	1.02		
2	1.03g	.5ml	2.06	2.1	0.00
	1.03g	.5ml	2.06		
	1.03g	.5ml	2.06		
2a	.17g	.1ml	1.7	1.7	0.00
	.17g	.1ml	1.7		
	.17g	.1ml	1.7		
3	.23g	.15ml	1.53	1.5	0.00
	.23g	.15ml	1.53		
	.23g	.15ml	1.53		
3a	.07g	.05ml	1.4	1.4	0.00
	.07g	.05ml	1.4		
	.07g	.05ml	1.4		
4	.38g	.25ml	1.52	1.5	0.00
	.38g	.25ml	1.52		
	.38g	.25ml	1.52		
5	.54g	.5ml	1.08	1.1	0.00
	.54g	.5ml	1.08		
	.54g	.5ml	1.08		
6	.60g	.4ml	1.5	1.5	0.00
	.60g	.4ml	1.5		
	.60g	.4ml	1.5		
7	.60g	.25ml	2.4	2.4	0.00
	.60g	.25ml	2.4		
	.60g	.25ml	2.4		
8	1.0g	.7ml	1.43	1.4	0.00
	1.0g	.7ml	1.43		
	1.0g	.7ml	1.43		
9	1.6g	1.0ml	1.6	1.6	0.00
	1.6g	1.0ml	1.6		
	1.6g	1.0ml	1.6		
10	1.4g	1.1ml	1.27	1.3	0.00
	1.3g	1.1ml	1.27		
	1.4g	1.1ml	1.27		
11	.95g	.7ml	1.36	1.4	0.00
	.95g	.7ml	1.36		
	.95g	.7ml	1.36		
12	.2g	.1ml	2	2.0	0.00
	.2g	.1ml	2		
	.2g	.1ml	2		
13	4.3g	3.0ml	1.43	1.5	0.06
	4.3g	2.8ml	1.54		
	4.3g	2.9ml	1.48		

TABLE 10.–Raw Data for Mass Density of Bone Pieces and Teeth (continued).

Bone #	Weight	Volume	Density	Ave Density	Std Dev
	grams	ml	g/ cm^3	g/ cm^3	
14	3.7g	2.6ml	1.42	1.4	0.00
	3.7g	2.6ml	1.42		
	3.7g	2.6ml	1.42		
15	2.9g	1.6ml	1.81	1.8	0.00
	2.9g	1.6ml	1.81		
	2.9g	1.6ml	1.81		
16	2.8g	1.4ml	2	2.0	0.08
	2.8g	1.5ml	1.87		
	2.8g	1.4ml	2		
17	.90g	.5ml	1.8	1.8	0.00
	.90g	.5ml	1.8		
	.90g	.5ml	1.8		
18	1.3g	1.0ml	1.3	1.3	0.00
	1.3g	1.0ml	1.3		
	1.3g	1.0ml	1.3		
20	1.8g	1.1ml	1.64	1.6	0.08
	1.8g	1.1ml	1.64		
	1.8g	1.2ml	1.5		
20a	1.1g	.8ml	1.4	1.5	0.10
	1.1g	.7ml	1.6		
	1.2g	.8ml	1.5		
21	1.8g	1.0ml	1.8	1.8	0.00
	1.8g	1.0ml	1.8		
	1.8g	1.0ml	1.8		
21a	1.1g	.6ml	1.8	1.8	0.00
	1.1g	.6ml	1.8		
	1.1g	.6ml	1.8		
22	1.2g	.9ml	1.3	1.4	0.12
	1.2g	.8ml	1.5		
	1.2g	.9ml	1.3		
22a	2.2g	1.1ml	2	1.9	0.10
	2.2g	1.2ml	1.83		
	2.2g	1.1ml	2		
23	2.5g	1.6ml	1.56	1.6	0.00
	2.5g	1.6ml	1.56		
	2.5g	1.6ml	1.56		
24	2.7g	2.0ml	1.35	1.4	0.00
	2.7g	2.0ml	1.35		
	2.7g	2.0ml	1.35		
25	2.2g	1.5ml	1.47	1.5	0.00
	2.2g	1.5ml	1.47		
	2.2g	1.5ml	1.47		
26	2.8g	1.9ml	1.47	1.5	0.00
	2.8g	1.9ml	1.47		
	2.8g	1.9ml	1.47		
30	2.8g	1.9ml	1.47	1.4	0.04
	2.8g	2.0ml	1.4		
	2.8g	1.9ml	1.47		
31	2.4g	1.4ml	1.71	1.7	0.04
	2.3g	1.4ml	1.64		
	2.4g	1.4ml	1.71		
32	2.7g	2.0ml	1.35	1.4	0.00
	2.7g	2.0ml	1.35		
	2.7g	2.0ml	1.35		
33	2.8g	1.8ml	1.56	1.6	0.00
	2.8g	1.8ml	1.56		
	2.8g	1.8ml	1.56		

TABLE 10.—Raw Data for Mass Density of Bone Pieces and Teeth (continued).

Bone #	Weight	Volume	Density	Ave Density	Std Dev
Units	grams	ml	g/ cm^3	g/ cm^3	
34	2.6g	1.7ml	1.53	1.5	0.00
	2.6g	1.7ml	1.53		
	2.6g	1.7ml	1.53		
35	2.9g	1.8ml	1.61	1.6	0.00
	2.9g	1.8ml	1.61		
	2.9g	1.8ml	1.61		
36	3.5g	2.3ml	1.52	1.5	0.00
	3.5g	2.3ml	1.52		
	3.5g	2.3ml	1.52		
40	.60g	.5ml	1.2	1.2	0.00
	.60g	.5ml	1.2		
	.60g	.5ml	1.2		
41	.15g	.1ml	1.5	1.5	0.00
	.15g	.1ml	1.5		
	.15g	.1ml	1.5		
42	1.9g	1.4ml	1.36	1.3	0.04
	1.9g	1.4ml	1.36		
	1.8g	1.4ml	1.29		
43	2.2g	1.7ml	1.29	1.3	0.04
	2.2g	1.7ml	1.29		
	2.2g	1.8ml	1.22		
44	1.4g	.8ml	1.75	1.8	0.00
	1.4g	.8ml	1.75		
	1.4g	.8ml	1.75		
45	1.9g	1.4ml	1.36	1.4	0.00
	1.9g	1.4ml	1.36		
	1.9g	1.4ml	1.36		
46	2.8g	2.0ml	1.4	1.4	0.00
	2.8g	2.0ml	1.4		
	2.8g	2.0ml	1.4		
47	2.0g	1.5ml	1.33	1.3	0.07
	1.9g	1.6ml	1.19		
	2.0g	1.6ml	1.25		
50	.60g	.5ml	1.2	1.2	0.00
	.60g	.5ml	1.2		
	.60g	.5ml	1.2		
51	.30g	.20ml	1.5	1.5	0.00
	.30g	.20ml	1.5		
	.30g	.20ml	1.5		
52	1.7g	1.1ml	1.55	1.6	0.00
	1.7g	1.1ml	1.55		
	1.7g	1.1ml	1.55		
53	2.5g	1.6ml	1.56	1.6	0.00
	2.5g	1.6ml	1.56		
	2.5g	1.6ml	1.56		
54	1.9g	1.2ml	1.58	1.6	0.00
	1.9g	1.2ml	1.58		
	1.9g	1.2ml	1.58		
55	1.8g	1.1ml	1.64	1.8	0.09
	1.8g	1.0ml	1.8		
	1.8g	1.0ml	1.8		
56	1.6g	1.0ml	1.6	1.7	0.06
	1.7g	1.0ml	1.7		
	1.7g	1.0ml	1.7		
57	1.4g	.8ml	1.75	1.8	0.00

TABLE 10.—Raw Data for Mass Density of Bone Pieces and Teeth (continued).

Bone # Units	Weight grams	Volume ml	Density g/ cm^3	Ave Density g/ cm^3	Std Dev
57	1.4g	.8ml			
	1.4g	.8ml			
60	1.3g	.8ml	1.63	1.6	0.00
	1.3g	.8ml	1.63		
	1.3g	.8ml	1.63		
61	.30g	.20ml	1.5	1.5	0.00
	.30g	.20ml	1.5		
	.30g	.20ml	1.5		
62	.50g	.40ml	1.25	1.4	0.24
	.50g	.30ml	1.67		
	.50g	.40ml	1.25		
63	.30g	.10ml	3	3.0	0.00
	.30g	.10ml	3		
	.30g	.10ml	3		
64	.50g	.2ml	2.5	2.5	0.00
	.50g	.2ml	2.5		
	.50g	.2ml	2.5		
65	.30g	.2ml	1.5	1.5	0.00
	.30g	.2ml	1.5		
	.30g	.2ml	1.5		
66	.80g	.5ml	1.6	1.5	0.16
	.80g	.6ml	1.33		
	.80g	.5ml	1.6		
67	.90g	.50ml	1.8	1.8	0.00
	.90g	.50ml	1.8		
	.90g	.50ml	1.8		
70	1.1g	.7ml	1.57	1.6	0.00
	1.1g	.7ml	1.57		
	1.1g	.7ml	1.57		
71	2.3g	1.7ml	1.35	1.4	0.00
	2.3g	1.7ml	1.35		
	2.3g	1.7ml	1.35		
72	3.4g	2.4ml	1.42	1.4	0.00
	3.4g	2.4ml	1.42		
	3.4g	2.4ml	1.42		
73	2.1g	1.5ml	1.4	1.4	0.06
	2.1g	1.4ml	1.5		
	2.1g	1.5ml	1.4		
74	1.7g	1.1ml	1.55	1.6	0.00
	1.7g	1.1ml	1.55		
	1.7g	1.1ml	1.55		
75	2.3g	1.7ml	1.35	1.4	0.00
	2.3g	1.7ml	1.35		
	2.3g	1.7ml	1.35		
76	1.1g	.60ml	1.83	1.8	0.00
	1.1g	.60ml	1.83		
	1.1g	.60ml	1.83		
77	1.4g	1.0ml	1.4	1.4	0.00
	1.4g	1.0ml	1.4		
	1.4g	1.0ml	1.4		
80	.70g	.50ml	1.4	1.4	0.00
	.70g	.50ml	1.4		
	.70g	.50ml	1.4		
81	4.9g	3.4ml	1.44	1.4	0.00
	4.9g	3.4ml	1.44		
	4.9g	3.4ml	1.44		
82	4.2g	3.4ml	1.24	1.2	0.00

TABLE 10.—Raw Data for Mass Density of Bone Pieces and Teeth (continued).

Bone #	Weight	Volume	Density	Ave Density	Std Dev
Units	grams	ml	g/ cm^3	g/ cm^3	
82	4.2g	3.4ml	1.24		
	4.2g	3.4ml	1.24		
83	1.6g	1.2ml	1.33	1.3	0.00
	1.6g	1.2ml	1.33		
	1.6g	1.2ml	1.33		
84	.90g	.70ml	1.29	1.3	0.00
	.90g	.70ml	1.29		
	.90g	.70ml	1.29		
85	2.7g	2.0ml	1.35	1.4	0.00
	2.7g	2.0ml	1.35		
	2.7g	2.0ml	1.35		
87	1.1g	.70ml	1.57	1.6	0.00
	1.1g	.70ml	1.57		
	1.1g	.70ml	1.57		
*mani	1.3g	.6ml	2.17	2.1	0.18
	1.3g	.7ml	1.86		
	1.3g	.6ml	2.17		
*manc	1.3g	.6ml	2.17	2.2	0.00
	1.3g	.6ml	2.17		
	1.3g	.6ml	2.17		
*manp	1.1g	.5ml	2.2	2.1	0.21
	1.1g	.6ml	1.83		
	1.1g	.5ml	2.2		
*maxi	1.1g	.5ml	2.2	2.2	0.00
	1.1g	.5ml	2.2		
	1.1g	.5ml	2.2		
*maxc	.8g	.4ml	2	2.0	0.00
	.8g	.4ml	2		
	.8g	.4ml	2		
*maxp	1.2g	.6ml	2	2.0	0.00
	1.2g	.6ml	2		
	1.2g	.6ml	2		

*mani- mandibular incisor, *manc- mandibular canine, *manp- mandibular premolar
*maxi- maxillary incisor, *maxc- maxillary canine, * maxc- maxillary premolar

TABLE 11.—Raw Data for Scanning Acoustic Microscope Readings of Bone and Teeth.

Bone #	Point #	SAM Voltage	Ave. Point Voltage	Point Voltage Std. Dev	Ave. Piece Voltage	Piece Voltage Std. Dev	Piece Modulus (GPa)
Steel		2.9					
1	1	1.6	1.4	0.09	1.7	0.19	26.2
		1.4					
		1.4					
		1.4					
		1.4					
	2	1.6	1.6	0.05			
		1.7					
		1.7					
		1.6					
		1.6					
	3	2.0	1.8	0.10			
		1.8					
		1.9					
		1.8					
		1.8					
	4	1.6	1.9	0.25			
		2.3					
		2.0					
		1.8					
		1.8					
Steel		3.5					
1a	1	0.6	0.9	0.57	1.3	0.52	9.4
		0.7					
		1.9					
		0.5					
		0.8					
	2	1.9	1.6	0.30			
		1.6					
		1.8					
		1.2					
		1.8					
Steel		2.8					
2	1	0.5	0.5	0.15	1.1	0.57	5.1
		0.4					
		0.7					
		0.4					
		0.3					
	2	1.4	1.5	0.09			
		1.5					
		1.6					
		1.4					
		1.5					
	3	1.2	1.4	0.32			
		1.3					
		1.2					
		1.4					
		2.0					

TABLE 11.—Raw Data for Scanning Acoustic Microscope Readings of Bone and Teeth (continued).

Bone #	Point #	SAM Voltage	Ave. Point Voltage	Point Voltage Std. Dev	Ave. Piece Voltage	Piece Voltage Std. Dev	Piece Modulus (GPa)
Steel		2.8					
2a	1	0.8	0.8	0.16	1.1	0.50	6.3
		0.8					
		1.0					
		0.6					
		0.6					
	2	1.5	1.5	0.07			
		1.5					
		1.6					
		1.4					
		1.4					
Steel		2.4					
3	1	0.8	0.9	0.07	0.9	0.00	6.4
		0.8					
		1.0					
		0.8					
		0.8					
3a	1	0.9	0.9	0.07	0.8	0.05	5.1
		0.8					
		0.9					
		0.8					
		0.9					
	2	0.8	0.8	0.04			
		0.8					
		0.8					
		0.7					
		0.8					
Steel		1.9					
4	1	0.8	0.9	0.11	0.7	0.25	6.2
		1.0					
		0.9					
		0.8					
		0.9					
	2	0.6	0.5	0.07			
		0.6					
		0.5					
		0.5					
		0.4					
Steel		1.6					
5	1	0.6	0.5	0.06	0.5	0.05	6.7
		0.5					
		0.5					
		0.4					
		0.4					
	2	0.6	0.6	0.03			
		0.6					
		0.6					
		0.6					
		0.6					
	3	0.5	0.6	0.05			
		0.6					
		0.6					
		0.5					
		0.6					

TABLE 11.—Raw Data for Scanning Acoustic Microscope Readings of Bone and Teeth (continued).

Bone #	Point #	SAM Voltage	Ave. Point Voltage	Point Voltage Std. Dev	Ave. Piece Voltage	Piece Voltage Std. Dev	Piece Modulus (GPa)
Steel		1.6					
6	1	0.8	0.8	0.28	0.8	0.17	11.3
		0.8					
		1.3					
		0.6					
		0.6					
	2	0.8	0.6	0.10			
		0.6					
		0.6					
		0.6					
		0.5					
	3	1.0	1.0	0.10			
		1.0					
		1.0					
		0.8					
		1.1					
Steel		2.4					
7	1	0.8	0.9	0.26	0.7	0.13	28.0
		1.0					
		1.2					
		0.6					
	2	0.6	0.6	0.07			
		0.7					
		0.5					
		0.6					
		0.6					
Steel		2.1					
8	1	1.1	1.1	0.06	1.4	0.02	29.8
		1.2					
		1.1					
		1.0					
		1.1					
	2	1.6	1.5	0.06			
		1.5					
		1.5					
		1.4					
		1.6					
	3	1.4	1.5	0.10			
		1.6					
		1.5					
		1.6					
		1.6					
Steel		2.3					
9	1	1.4	1.4	0.05	1.4	0.02	20.0
		1.4					
		1.4					
		1.5					
		1.5					
	2	1.5	1.5	0.12			
		1.6					
		1.6					
		1.4					
		1.4					
	3	1.2	1.4	0.21			
		1.5					
		1.5					
		1.3					
		1.8					

TABLE 11.—Raw Data for Scanning Acoustic Microscope Readings of Bone and Teeth (continued).

Bone #	Point #	SAM Voltage	Ave. Point Voltage	Point Voltage Std. Dev	Ave. Piece Voltage	Piece Voltage Std. Dev	Piece Modulus (GPa)
Steel		2.4					
10	1	1.5	1.4	0.04	1.4	0.01	19.9
		1.4					
		1.4					
		1.5					
		1.4					
	2	1.5	1.4	0.04			
		1.4					
		1.4					
		1.4					
		1.5					
Steel		2.9					
11	1	1.5	1.6	0.23	1.5	0.27	13.1
		2.0					
		1.4					
		1.8					
		1.5					
	2	1.8	1.8	0.08			
		2.0					
		1.9					
		1.8					
		1.8					
	3	0.9	1.2	0.32			
		0.9					
		1.3					
		1.5					
		1.5					
	4	1.5	1.5	0.14			
		1.8					
		1.4					
		1.5					
		1.5					
Steel		2.9					
12	1	1.6	1.8	0.15	1.8	0.00	15.9
		1.8					
		2.0					
		2.0					
		1.9					

TABLE 11.—Raw Data for Scanning Acoustic Microscope Readings of Bone and Teeth (continued).

Bone #	Point#	SAM Voltage	Ave. Point Voltage	Point Voltage Std. Dev	Ave. Piece Voltage	Piece Voltage Std. Dev	Piece Modulus (GPa)
Steel		1.9					
13	1	1.4	1.5	0.16	2.2	0.81	47.3
		1.8					
		1.5					
		1.4					
		1.4					
	2	1.4	1.5	0.34			
		1.3					
		2.0					
		1.2					
		1.8					
	3	1.5	2.8	0.76			
		2.9					
		3.5					
		3.1					
		3.0					
	4	2.8	3.0	0.16			
		3.1					
		3.2					
		3.0					
		3.0					
Steel		1.9					
14	1	2.0	1.6	0.39	1.6	0.12	147.4
		1.9					
		1.6					
		1.8					
		1.0					
	2	1.9	1.7	0.29			
		1.3					
		2.0					
		1.6					
		1.6					
	3	1.5	1.4	0.07			
		1.5					
		1.4					
		1.3					
		1.4					
	4	1.5	1.6	0.40			
		1.6					
		1.0					
		2.0					
		2.0					

TABLE 11.—Raw Data for Scanning Acoustic Microscope Readings of Bone and Teeth (continued).

Bone #	Point #	SAM Voltage	Ave. Point Voltage	Point Voltage Std. Dev	Ave. Piece Voltage	Piece Voltage Std. Dev	Piece Modulus (GPa)
Steel		2.0					
15	1	0.7	0.6	0.12	1.0	0.59	9.4
		0.8					
		0.5					
		0.6					
		0.6					
	2	0.6	0.5	0.05			
		0.5					
		0.5					
		0.5					
		0.6					
	3	2.0	1.8	0.32			
		2.0					
		2.0					
		2.0					
		1.3					
	4	1.1	1.1	0.13			
		1.3					
		1.0					
		1.3					
		1.0					
Steel		2.0					
16	1	1.9	1.8	0.07	1.8	0.18	157.8
		1.8					
		1.9					
		1.8					
		1.8					
	2	2.0	1.9	0.05			
		2.0					
		2.0					
		2.0					
		1.9					
	3	2.0	1.8	0.10			
		1.9					
		1.8					
		1.9					
		1.7					
	4	1.9	1.5	0.21			
		1.5					
		1.5					
		1.3					
		1.6					

TABLE 11.—Raw Data for Scanning Acoustic Microscope Readings of Bone and Teeth (continued).

Bone #	Point #	SAM Voltage	Ave. Point Voltage	Point Voltage Std. Dev	Ave. Piece Voltage	Piece Voltage Std. Dev	Piece Modulus (GPa)
Steel		2.0					
17	1	1.5	1.5	0.06	1.5	0.08	40.8
		1.6					
		1.4					
		1.5					
		1.5					
	2	1.5	1.5	0.04			
		1.5					
		1.6					
		1.6					
		1.6					
	3	1.7	1.6	0.06			
		1.6					
		1.6					
		1.6					
		1.5					
	4	1.5	1.4	0.14			
		1.3					
		1.6					
		1.3					
		1.4					
Steel		2.5					
18	1	1.9	1.9	0.04	1.7	0.18	34.9
		1.9					
		2.0					
		1.9					
		1.9					
	2	1.8	1.8	0.04			
		1.9					
		1.9					
		1.9					
		1.8					
	3	1.4	1.8	0.22			
		1.9					
		1.9					
		1.9					
		1.9					
	4	1.6	1.5	0.10			
		1.6					
		1.4					
		1.4					
		1.5					
Steel		2.7					
20	1	2.0	2.1	0.16	2.0	0.15	42.8
		2.3					
		2.0					
		2.2					
		2.3					
	2	1.8	1.9	0.34			
		1.8					
		1.5					
		2.3					
		2.3					

TABLE 11.—Raw Data for Scanning Acoustic Microscope Readings of Bone and Teeth (continued).

Bone #	Point #	SAM Voltage	Ave. Point Voltage	Point Voltage Std. Dev	Ave. Piece Voltage	Piece Voltage Std. Dev	Piece Modulus (GPa)
Steel		2.7					
20a	1	2.2	2.0	0.18	2.1	0.16	60.7
		1.8					
		2.3					
		2.0					
		1.9					
	2	2.4	2.3	0.11			
		2.2					
		2.1					
		2.3					
		2.4					
Steel		2.6					
21	1	1.9	1.9	0.05	2.0	0.11	47.2
		1.9					
		2.0					
		2.0					
		2.0					
	2	2.0	2.1	0.13			
		2.0					
		2.2					
		2.3					
		2.0					
Steel		2.6					
21a	1	1.6	2.0	0.23	2.0	0.09	47.2
		2.2					
		2.1					
		2.0					
		2.0					
	2	2.2	2.1	0.08			
		2.2					
		2.1					
		2.0					
		2.1					
Steel		2.5					
22	1	1.7	1.7	0.09	1.9	0.24	56.5
		1.8					
		1.8					
		1.6					
		1.7					
	2	2.1	2.0	0.11			
		2.0					
		1.9					
		2.2					
		2.2					
Steel		2.5					
22a	1	1.9	2.0	0.13	1.8	0.21	31.1
		2.1					
		2.0					
		2.2					
		1.9					
	2	1.7	1.7	0.11			
		1.8					
		1.5					
		1.8					
		1.7					

TABLE 11.—Raw Data for Scanning Acoustic Microscope Readings of Bone and Teeth (continued).

Bone #	Point #	SAM Voltage	Ave. Point Voltage	Point Voltage Std. Dev	Ave. Piece Voltage	Piece Voltage Std. Dev	Piece Modulus (GPa)
Steel		2.5					
23	1	1.9	1.8	0.19	1.6	0.10	22.2
		1.9					
		1.6					
		1.9					
		1.5					
	2	1.9	1.6	0.24			
		1.5					
		1.9					
		1.4					
		1.5					
	3	1.5	1.6	0.26			
		1.3					
		2.0					
		1.7					
		1.5					
	4	1.5	1.5	0.30			
		1.7					
		1.3					
		1.3					
		2.0					
Steel		2.5					
24	1	1.5	1.5	0.16	1.7	0.21	32.3
		1.3					
		1.4					
		1.7					
		1.6					
	2	2.0	1.8	0.11			
		1.8					
		1.8					
		1.9					
		1.8					
	3	1.8	1.5	0.22			
		1.5					
		1.3					
		1.3					
		1.4					
	4	1.9	1.9	0.17			
		2.0					
		1.6					
		1.9					
		2.1					

TABLE 11.—Raw Data for Scanning Acoustic Microscope Readings of Bone and Teeth (continued).

Bone #	Point #	SAM Voltage	Ave. Point Voltage	Point Voltage Std. Dev	Ave. Piece Voltage	Piece Voltage Std. Dev	Piece Modulus (GPa)
Steel		2.9					
25	1	0.9	0.8	0.05	0.9	0.22	4.9
		0.9					
		0.8					
		0.9					
		0.9					
	2	1.2	1.2	0.42			
		0.8					
		1.5					
		0.9					
		1.8					
	3	0.7	0.8	0.11			
		0.7					
		0.8					
		0.8					
		1.0					
	4	0.7	0.8	0.19			
		0.7					
		0.8					
		0.8					
		1.1					
Steel		2.9					
26	1	2.0	2.0	0.00	1.8	0.16	21.2
		2.0					
		2.0					
		2.0					
		2.0					
	2	2.0	1.6	0.32			
		1.4					
		2.0					
		1.3					
		1.4					
	3	1.8	1.7	0.35			
		1.9					
		1.9					
		1.2					
	4	1.9	1.9	0.18			
		1.9					
		1.9					
		2.1					
		1.6					

TABLE 11.—Raw Data for Scanning Acoustic Microscope Readings of Bone and Teeth (continued).

Bone #	Point #	SAM Voltage	Ave. Point Voltage	Point Voltage Std. Dev	Ave. Piece Voltage	Piece Voltage Std. Dev	Piece Modulus (GPa)
Steel		2.5					
30	1	1.8	1.8	0.15	1.5	0.30	20.2
		2.0					
		1.6					
		1.8					
		2.0					
	2	1.3	1.3	0.03			
		1.3					
		1.3					
		1.3					
		1.3					
	3	1.2	1.2	0.15			
		1.4					
		1.0					
		1.2					
		1.3					
	4	1.8	1.7	0.21			
		1.4					
		1.8					
		1.6					
		1.9					
Steel		2.5					
31	1	0.9	0.8	0.07	1.4	0.51	13.4
		0.9					
		0.9					
		0.8					
		0.8					
	2	2.0	2.0	0.11			
		2.0					
		2.1					
		1.9					
		2.1					
	3	0.8	1.1	0.23			
		1.3					
		1.0					
		1.3					
		1.3					
	4	1.2	1.6	0.36			
		1.7					
		2.2					
		1.6					
		1.6					

TABLE 11.—Raw Data for Scanning Acoustic Microscope Readings of Bone and Teeth (continued).

Bone#	Point #	SAM Voltage	Ave. Point Voltage	Point Voltage Std. Dev	Ave. Piece Voltage	Piece Voltage Std. Dev	Piece Modulus (GPa)
32	1	1.7	1.6	0.18	1.4	0.35	19.7
		1.8					
		1.9					
		1.4					
		1.5					
	2	1.5	1.6	0.20			
		2.0					
		1.5					
		1.7					
		1.6					
	3	1.1	0.9	0.13			
		0.9					
		1.0					
		0.8					
		0.9					
	4	1.7	1.6	0.26			
		1.4					
		1.9					
		1.8					
		1.3					
Steel		2.4					
33	1	2.0	1.7	0.17	1.9	0.22	73.8
		1.5					
		1.6					
		1.7					
		1.6					
	2	1.9	1.7	0.19			
		1.7					
		1.7					
		1.9					
		1.4					
	3	2.0	2.0	0.08			
		2.0					
		1.9					
		2.1					
		2.0					
	4	2.3	2.1	0.22			
		2.3					
		1.8					
		2.3					
		2.0					

TABLE 11.—Raw Data for Scanning Acoustic Microscope Readings of Bone and Teeth (continued).

Bone #	Point #	SAM Voltage	Ave. Point Voltage	Point Voltage Std. Dev	Ave. Piece Voltage	Piece Voltage Std. Dev	Piece Modulus (GPa)
Steel		2.4					
34	1	2.2	2.0	0.12	1.6	0.44	30.4
		1.8					
		2.0					
		2.0					
		2.0					
	2	1.9	1.9	0.08			
		1.9					
		1.9					
		1.9					
		2.1					
	3	0.9	1.3	0.36			
		0.9					
		1.6					
		1.6					
		1.4					
	4	1.0	1.1	0.17			
		1.0					
		1.3					
		1.3					
		1.0					
Steel		2.4					
35	1	1.3	1.5	0.27	1.6	0.30	28.5
		2.0					
		1.4					
		1.5					
		1.4					
	2	2.0	1.8	0.13			
		1.8					
		1.7					
		1.8					
		2.0					
	3	1.9	1.9	0.07			
		2.0					
		2.0					
		1.9					
		1.9					
	4	1.5	1.5	0.00			
		1.5					
		1.5					
		1.5					
		1.5					
	5	1.0	1.1	0.07			
		1.2					
		1.1					
		1.0					
		1.1					
	6	1.8	1.6	0.11			
		1.5					
		1.6					
		1.6					
		1.6					

TABLE 11.—Raw Data for Scanning Acoustic Microscope Readings of Bone and Teeth (continued).

Bone #	Point #	SAM Voltage	Ave. Point Voltage	Point Voltage Std. Dev	Ave. Piece Voltage	Piece Voltage Std. Dev	Piece Modulus (GPa)
Steel		2.6					
36	1	2.2	2.2	0.07	1.7	0.08	25.7
		2.3					
		2.2					
		2.3					
		2.1					
	2	1.5	1.7	0.16			
		1.8					
		2.0					
		1.8					
		1.7					
	3	1.2	1.2	0.10			
		1.3					
		1.2					
		1.1					
		1.1					
	4	1.5	1.3	0.19			
		1.4					
		1.5					
		1.3					
		1.1					
	5	1.9	1.7	0.21			
		1.6					
		1.9					
		1.7					
		1.4					
	6	1.6	2.0	0.27			
		2.0					
		1.8					
		2.3					
		2.2					
Steel		2.5					
40	1	2.0	1.8	0.24	1.8	0.40	54.7
		2.0					
		2.0					
		1.4					
		1.8					
	2	2.2	2.2	0.08			
		2.3					
		2.2					
		2.3					
		2.4					
	3	1.3	1.4	0.12			
		1.4					
		1.5					
		1.6					
		1.5					
Steel		2.5					
41	1	1.5	1.8	0.28	1.7	0.13	33.1
		1.9					
		1.5					
		2.0					
		2.1					
	2	1.8	1.6	0.39			
		1.6					
		1.0					
		2.1					
		1.5					

TABLE 11.—Raw Data for Scanning Acoustic Microscope Readings of Bone and Teeth (continued).

Bone #	Point #	SAM Voltage	Ave. Point Voltage	Point Voltage Std. Dev	Ave. Piece Voltage	Piece Voltage Std. Dev	Piece Modulus (GPa)
Steel		2.5					
42	1	2.1	2.0	0.24	1.8	0.08	50.4
		2.0					
		2.3					
		1.7					
		2.1					
	2	1.8	2.0	0.13			
		2.0					
		2.0					
		2.2					
		2.0					
		2.0					
	3	1.8	1.5	0.18			
		1.5					
		1.3					
		1.6					
		1.6					
	4	1.4	1.6	0.33			
		1.3					
		1.8					
		2.1					
		1.8					
Steel		2.5					
43	1	1.6	1.6	0.19	1.7	0.19	38.1
		2.0					
		1.5					
		1.7					
		1.5					
	2	1.8	1.7	0.13			
		1.8					
		1.9					
		1.8					
		1.5					
	3	1.8	1.5	0.26			
		1.9					
		1.3					
		1.4					
		1.5					
	4	2.0	2.0	0.06			
		2.0					
		2.0					
		1.9					
		2.1					

TABLE 11.—Raw Data for Scanning Acoustic Microscope Readings of Bone and Teeth (continued).

Bone #	Point #	SAM Voltage	Ave. Point Voltage	Point Voltage Std. Dev	Ave. Piece Voltage	Piece Voltage Std. Dev	Piece Modulus (GPa)
Steel		2.5					
44	1	2.1	2.0	0.11	2.0	0.11	70.4
		2.2					
		1.9					
		2.1					
		2.1					
	2	2.1	2.1	0.18			
		2.1					
		2.3					
		2.1					
		1.8					
	3	1.7	1.8	0.22			
		2.0					
		2.0					
		1.5					
		1.9					
	4	2.0	2.0	0.07			
		2.1					
		1.9					
		1.9					
		2.0					
Steel		2.7					
45	1	2.0	2.0	0.20	1.9	0.21	41.4
		2.3					
		2.1					
		1.8					
		1.8					
	2	2.3	1.9	0.38			
		1.8					
		1.5					
		1.5					
		2.3					
	3	2.2	2.2	0.11			
		2.3					
		2.0					
		2.1					
		2.3					
	4	2.2	1.7	0.28			
		1.6					
		1.5					
		1.5					
		1.6					

TABLE 11.—Raw Data for Scanning Acoustic Microscope Readings of Bone and Teeth (continued).

Bone #	Point #	SAM Voltage	Ave. Point Voltage	Point Voltage Std. Dev	Ave. Piece Voltage	Piece Voltage Std. Dev	Piece Modulus (GPa)
Steel		2.7					
46	1	2.0	2.0	0.09	1.9	0.13	41.4
		2.1					
		2.1					
		1.9					
		2.2					
	2	1.9	1.8	0.25			
		1.6					
		2.1					
		1.9					
		1.5					
	3	2.2	2.0	0.08			
		2.0					
		2.0					
		2.1					
		2.0					
	4	2.0	1.9	0.07			
		1.9					
		1.9					
		1.9					
		1.9					
Steel		2.5					
47	1	2.0	2.0	0.20	2.1	0.09	122.2
		1.8					
		2.1					
		2.1					
		2.3					
	2	2.2	2.1	0.06			
		2.0					
		2.1					
		2.0					
		2.1					
	3	2.3	2.2	0.08			
		2.3					
		2.2					
		2.2					
		2.1					
	4	1.8	2.0	0.14			
		2.0					
		2.0					
		2.1					
		2.1					
Steel		2.5					
50	1	1.6	1.9	0.16	2.0	0.08	91.3
		2.0					
		2.0					
		2.0					
		2.0					
	2	2.2	2.0	0.08			
		2.0					
		2.0					
		2.0					
		2.0					
	3	2.0	2.0	0.11			
		2.2					
		2.0					
		2.0					
		2.0					

TABLE 11.—Raw Data for Scanning Acoustic Microscope Readings of Bone and Teeth (continued).

Bone #	Point #	SAM Voltage	Ave. Point Voltage	Point Voltage Std. Dev	Ave. Piece Voltage	Piece Voltage Std. Dev	Piece Modulus (GPa)
Steel		2.5					
51	1	2.0	2.0	0.08	2.1	0.11	105.9
		2.0					
		2.1					
		1.9					
		2.1					
	2	1.8	2.1	0.20			
		2.3					
		2.3					
		2.3					
		2.1					
Steel		2.7					
52	1	2.3	2.2	0.19	2.1	0.06	64.2
		2.0					
		2.0					
		2.5					
		2.3					
	2	2.0	2.1	0.18			
		2.3					
		2.4					
		2.0					
		2.1					
	3	2.3	2.2	0.05			
		2.3					
		2.3					
		2.3					
		2.2					
	4	2.0	2.1	0.15			
		2.3					
		1.9					
		2.1					
		2.1					
Steel		2.7					
53	1	2.3	2.2	0.16	2.0	0.21	47.5
		2.3					
		2.3					
		1.9					
		2.3					
	2	2.1	2.0	0.14			
		2.1					
		1.8					
		2.1					
		2.0					
	3	2.1	2.1	0.16			
		1.9					
		2.3					
		2.3					
		2.0					
	4	1.8	1.7	0.07			
		1.8					
		1.8					
		1.6					
		1.7					

TABLE 11.—Raw Data for Scanning Acoustic Microscope Readings of Bone and Teeth (continued).

Bone #	Point #	SAM Voltage	Ave. Point Voltage	Point Voltage Std. Dev	Ave. Piece Voltage	Piece Voltage Std. Dev	Piece Modulus (GPa)
Steel		2.7					
54	1	2.3	2.2	0.12	2.1	0.12	64.2
		2.3					
		2.3					
		2.1					
		2.0					
	2	2.3	2.0	0.13			
		2.0					
		1.9					
		2.1					
		2.0					
	3	2.3	2.2	0.18			
		2.3					
		2.3					
		1.9					
		2.3					
	4	1.7	1.9	0.22			
		2.1					
		2.0					
		1.7					
		2.2					
Steel		2.7					
55	1	2.1	2.0	0.04	2.0	0.10	42.2
		2.0					
		2.0					
		2.1					
		2.0					
	2	2.0	2.0	0.10			
		2.1					
		2.2					
		2.0					
		2.0					
	3	1.9	2.1	0.14			
		2.1					
		2.3					
		2.3					
		2.1					
	4	2.0	1.9	0.11			
		2.0					
		2.0					
		1.7					
		1.9					

TABLE 11.—Raw Data for Scanning Acoustic Microscope Readings of Bone and Teeth (continued).

Bone #	Point #	SAM Voltage	Ave. Point Voltage	Point Voltage Std. Dev	Ave. Piece Voltage	Piece Voltage Std. Dev	Piece Modulus (GPa)
Steel		2.7					
56	1	2.1	2.1	0.08	1.9	0.19	34.1
		2.1					
		2.2					
		2.2					
		2.0					
	2	1.9	1.8	0.15			
		2.0					
		1.9					
		1.6					
		1.7					
	3	1.7	1.7	0.16			
		1.8					
		1.8					
		1.7					
		1.4					
	4	2.1	2.0	0.20			
		1.9					
		2.3					
		1.8					
		1.8					
Steel		2.7					
57	1	1.4	1.6	0.17	2.0	0.26	42.2
		1.9					
		1.5					
		1.6					
		1.6					
	2	1.9	2.0	0.14			
		2.0					
		2.3					
		2.0					
		2.0					
	3	2.1	2.2	0.08			
		2.1					
		2.2					
		2.3					
		2.2					
	4	2.1	2.1	0.10			
		2.3					
		2.1					
		2.1					
		2.0					

TABLE 11.—Raw Data for Scanning Acoustic Microscope Readings of Bone and Teeth (continued).

Bone #	Point #	SAM Voltage	Ave. Point Voltage	Point Voltage Std. Dev	Ave. Piece Voltage	Piece Voltage Std. Dev	Piece Modulus (GPa)
Steel		2.5					
60	1	1.5	1.5	0.08	1.6	0.14	24.0
		1.5					
		1.6					
		1.4					
		1.4					
	2	1.7	1.6	0.16			
		1.4					
		1.8					
		1.6					
		1.8					
	3	2.0	1.8	0.13			
		1.7					
		1.7					
		1.8					
		1.9					
	4	1.6	1.5	0.13			
		1.6					
		1.7					
		1.4					
		1.4					
Steel		2.5					
61	1	2.0	1.9	0.09	1.9	0.02	59.6
		2.0					
		1.8					
		1.9					
		2.0					
	2	2.0	1.9	0.06			
		1.9					
		1.9					
		2.0					
		1.9					
62	1	1.9	2.1	0.16	2.1	0.02	135.5
		2.3					
		2.1					
		2.2					
		2.0					
	2	2.1	2.1	0.03			
		2.1					
		2.1					
		2.1					
		2.1					
Steel		2.8					
63	1	2.0	2.1	0.20	1.9	0.29	16.2
		2.1					
		2.1					
		2.5					
		2.0					
	2	2.0	1.7	0.17			
		1.6					
		1.8					
		1.6					
		1.6					

TABLE 11.—Raw Data for Scanning Acoustic Microscope Readings of Bone and Teeth (continued).

Bone #	Point #	SAM Voltage	Ave. Point Voltage	Point Voltage Std. Dev	Ave. Piece Voltage	Piece Voltage Std. Dev	Piece Modulus (GPa)
Steel		2.8					
64	1	2.1	2.1	0.10	2.0	0.05	24.9
		2.0					
		2.1					
		2.0					
		2.3					
	2	2.0	2.0	0.14			
		1.9					
		2.0					
		2.3					
		2.0					
Steel		2.8					
65	1	2.0	2.0	0.10	2.1	0.16	68.5
		2.0					
		1.9					
		2.1					
		2.2					
	2	2.4	2.2	0.16			
		2.2					
		2.0					
		2.4					
		2.4					
Steel		2.7					
66	1	2.1	2.0	0.08	1.8	0.16	30.1
		2.0					
		2.0					
		1.9					
		1.9					
	2	2.1	2.0	0.08			
		2.0					
		2.0					
		1.9					
		1.9					
	3	2.0	1.9	0.07			
		1.9					
		1.9					
		1.8					
		1.8					
	4	1.6	1.6	0.05			
		1.7					
		1.6					
		1.6					
		1.6					

TABLE 11.—Raw Data for Scanning Acoustic Microscope Readings of Bone and Teeth (continued).

Bone #	Point #	SAM Voltage	Ave. Point Voltage	Point Voltage Std. Dev	Ave. Piece Voltage	Piece Voltage Std. Dev	Piece Modulus (GPa)
Steel		2.7					
67	1	1.8	1.8	0.25	1.8	0.17	25.1
		2.3					
		1.7					
		1.8					
		1.7					
	2	1.9	1.8	0.17			
		1.9					
		2.0					
		1.7					
		1.6					
	3	1.7	1.5	0.10			
		1.6					
		1.5					
		1.4					
		1.5					
	4	2.0	1.9	0.04			
		1.9					
		1.9					
		2.0					
		1.9					
Steel		2.3					
70	1	1.5	1.6	0.24	1.6	0.08	31.4
		1.5					
		2.0					
		1.8					
		1.4					
	2	1.6	1.5	0.13			
		1.5					
		1.6					
		1.5					
		1.3					
	3	1.7	1.6	0.19			
		1.7					
		1.3					
		1.7					
		1.8					
Steel		2.4					
71	1	2.0	2.0	0.05	1.8	0.10	52.4
		2.0					
		2.0					
		1.9					
		1.9					
	2	1.9	1.8	0.13			
		1.9					
		1.9					
		1.6					
		1.7					
	3	1.8	1.8	0.19			
		2.1					
		1.6					
		1.6					
		1.8					

TABLE 11.—Raw Data for Scanning Acoustic Microscope Readings of Bone and Teeth (continued).

Bone #	Point #	SAM Voltage	Ave. Point Voltage	Point Voltage Std. Dev	Ave. Piece Voltage	Piece Voltage Std. Dev	Piece Modulus (GPa)
Steel		2.4					
72	1	1.4	1.5	0.04	1.5	0.26	23.2
		1.5					
		1.5					
		1.5					
		1.5					
	2	1.4	1.3	0.08			
		1.4					
		1.3					
		1.3					
		1.3					
	3	1.3	1.3	0.08			
		1.4					
		1.3					
		1.5					
		1.3					
	4	2.0	1.9	0.16			
		2.0					
		2.0					
		1.6					
		1.9					
Steel		2.3					
73	1	2.0	1.7	0.18	1.5	0.16	29.7
		1.6					
		1.6					
		1.6					
		1.7					
	2	1.3	1.4	0.08			
		1.4					
		1.5					
		1.4					
		1.5					
	3	1.4	1.4	0.25			
		1.5					
		1.4					
		1.1					
		1.8					
	4	1.3	1.3	0.11			
		1.5					
		1.2					
		1.3					
		1.3					

TABLE 11.—Raw Data for Scanning Acoustic Microscope Readings of Bone and Teeth (continued).

Bone #	Point #	SAM Voltage	Ave. Point Voltage	Point Voltage Std. Dev	Ave. Piece Voltage	Piece Voltage Std. Dev	Piece Modulus (GPa)
Steel		2.9					
74	1	1.1	1.0	0.07	1.4	0.26	9.7
		1.0					
		1.1					
		1.1					
		1.0					
	2	1.6	1.6	0.19			
		1.9					
		1.5					
		1.5					
		1.5					
	3	1.4	1.3	0.16			
		1.2					
		1.5					
		1.2					
		1.5					
	4	1.5	1.6	0.08			
		1.6					
		1.6					
		1.7					
		1.6					
Steel		2.9					
75	1	1.9	1.7	0.21	1.7	0.10	18.7
		1.9					
		1.4					
		1.5					
		1.8					
	2	1.9	1.7	0.21			
		1.9					
		1.5					
		1.9					
		1.5					
	3	2.0	1.8	0.17			
		1.7					
		1.7					
		2.0					
		1.9					
	4	2.0	1.6	0.20			
		1.5					
		1.5					
		1.5					
		1.6					

TABLE 11.—Raw Data for Scanning Acoustic Microscope Readings of Bone and Teeth (continued).

Bone #	Point #	SAM Voltage	Ave. Point Voltage	Point Voltage Std. Dev	Ave. Piece Voltage	Piece Voltage Std. Dev	Piece Modulus (GPa)
Steel		2.9					
76	1	1.4	1.5	0.27	1.3	0.19	7.3
		1.4					
		2.0					
		1.4					
		1.4					
	2	1.1	1.1	0.04			
		1.1					
		1.0					
		1.1					
		1.1					
	3	1.5	1.4	0.08			
		1.4					
		1.6					
		1.4					
		1.4					
	4	1.0	1.3	0.27			
		1.6					
		1.5					
		1.4					
		1.2					
Steel		2.9					
77	1	1.6	1.6	0.19	1.6	0.18	16.4
		1.6					
		1.4					
		1.5					
		1.9					
	2	1.5	1.4	0.13			
		1.5					
		1.4					
		1.4					
		1.2					
	3	1.4	1.6	0.20			
		1.5					
		1.6					
		1.5					
		1.9					
	4	1.6	1.8	0.17			
		2.0					
		1.9					
		1.7					
		2.0					
Steel		2.9					
80	1	1.9	1.6	0.31	1.4	0.23	11.1
		2.0					
		1.4					
		1.3					
		1.4					
	2	1.1	1.2	0.14			
		1.2					
		1.0					
		1.2					
		1.4					
	3	1.3	1.5	0.23			
		1.4					
		1.9					
		1.5					
		1.4					

TABLE 11.—Raw Data for Scanning Acoustic Microscope Readings of Bone and Teeth (continued).

Bone #	Point #	SAM Voltage	Ave. Point Voltage	Point Voltage Std. Dev	Ave. Piece Voltage	Piece Voltage Std. Dev	Piece Modulus (GPa)
Steel		2.8					
81	1	1.5	1.4	0.06	1.6	0.22	18.3
		1.4					
		1.4					
		1.4					
		1.4					
	2	1.4	1.6	0.33			
		1.6					
		2.0					
		2.0					
		1.3					
	3	1.8	1.8	0.24			
		2.0					
		1.5					
		2.0					
		2.0					
Steel		2.8					
82	1	1.8	1.6	0.13	1.4	0.17	14.7
		1.5					
		1.5					
		1.7					
		1.8					
	2	1.9	1.5	0.48			
		2.0					
		1.0					
		1.0					
		1.4					
	3	1.5	1.3	0.23			
		1.2					
		1.5					
		1.1					
		1.0					
	4	1.3	1.3	0.47			
		0.9					
		1.0					
		2.1					
		1.3					
Steel		3.0					
83	1	1.9	1.9	0.16	1.8	0.15	21.7
		2.0					
		2.0					
		1.8					
		1.6					
	2	1.4	1.9	0.27			
		2.0					
		2.0					
		2.0					
		2.0					
	3	1.3	1.6	0.28			
		2.0					
		1.5					
		1.6					
		1.5					
	4	1.5	1.8	0.46			
		1.5					
		1.5					
		2.0					
		2.5					

TABLE 11.—Raw Data for Scanning Acoustic Microscope Readings of Bone and Teeth (continued).

Bone #	Point #	SAM Voltage	Ave. Point Voltage	Point Voltage Std. Dev	Ave. Piece Voltage	Piece Voltage Std. Dev	Piece Modulus (GPa)
Steel		3.0					
84	1	2.1	1.9	0.39	1.8	0.16	21.7
		2.2					
		1.2					
		2.0					
		1.9					
	2	1.9	2.0	0.20			
		2.0					
		1.7					
		2.2					
		2.1					
	3	1.6	1.6	0.22			
		1.4					
		1.5					
		1.9					
		1.9					
	4	2.0	1.7	0.17			
		1.6					
		1.7					
		1.5					
		1.6					
Steel		3.0					
85	1	1.5	1.5	0.32	1.6	0.11	14.2
		1.6					
		1.0					
		1.5					
		1.9					
	2	1.6	1.7	0.16			
		1.6					
		1.7					
		1.9					
		2.0					
	3	1.7	1.6	0.34			
		1.5					
		1.7					
		1.0					
		1.9					
	4	1.8	1.7	0.15			
		2.0					
		1.6					
		1.6					
		1.6					

TABLE 11.—Raw Data for Scanning Acoustic Microscope Readings of Bone and Teeth (continued).

Bone #	Point #	SAM Voltage	Ave. Point Voltage	Point Voltage Std. Dev	Ave. Piece Voltage	Piece Voltage Std. Dev	Piece Modulus (GPa)
Steel		2.8					
87	1	1.9	1.9	0.08	1.7	0.14	19.6
		1.9					
		1.9					
		1.8					
		2.0					
	2	1.8	1.7	0.18			
		1.9					
		1.5					
		1.8					
		1.5					
	3	1.5	1.6	0.07			
		1.6					
		1.5					
		1.5					
		1.7					
	4	1.8	1.6	0.13			
		1.5					
		1.5					
		1.5					
		1.6					
*mani	1	2.2	2.2	0.09	2.4	0.18	107.4
		2.4					
		2.3					
		2.1					
		2.2					
	2	2.5	2.5	0.14			
		2.5					
		2.3					
		2.6					
		2.6					
Steel		2.8					
*manc	1	2.6	2.6	0.04	2.6	0.01	287.6
		2.6					
		2.7					
		2.7					
		2.6					
	2	2.7	2.6	0.03			
		2.7					
		2.6					
		2.7					
		2.6					
Steel		2.7					
*manp	1	2.7	2.7	0.04	2.6	0.05	301.3
		2.7					
		2.7					
		2.6					
		2.7					
	2	2.7	2.6	0.10			
		2.6					
		2.7					
		2.5					
		2.5					

TABLE 11.—Raw Data for Scanning Acoustic Microscope Readings of Bone and Teeth (continued).

Bone #	Point #	SAM Voltage	Ave. Point Voltage	Point Voltage Std. Dev	Ave. Piece Voltage	Piece Voltage Std. Dev	Piece Modulus (GPa)
Steel		2.8					
*maxl	1	2.6	2.6	0.03	2.7	0.04	621.1
		2.6					
		2.6					
		2.7					
		2.7					
	2	2.7	2.7	0.03			
		2.7					
		2.7					
		2.7					
		2.7					
Steel		2.8					
*maxc	1	2.8	2.7	0.04	2.6	0.11	316.3
		2.8					
		2.7					
		2.7					
		2.7					
	2	2.7	2.6	0.13			
		2.4					
		2.5					
		2.7					
		2.7					
Steel		2.8					
*maxp	1	2.6	2.6	0.03	2.6	0.01	316.3
		2.7					
		2.7					
		2.6					
		2.7					
	2	2.7	2.6	0.04			
		2.7					
		2.7					
		2.6					
		2.6					

*mani- mandibular incisor, *manc- mandibular canine, *manp- mandibular premolar
*maxi- maxillary incisor, *maxc- maxillary canine, *maxp- maxillary premolar

TABLE 12.–Raw Data for Vicker's Hardness (H_v) for Bone Pieces and Teeth.

Bone #	Point #	Vicker's Hardness	Ave. Point H_v	Point H_v Std. Dev	Ave. Piece H_v	Piece H_v Std. Dev
1	1	60.3	49.1	13.1	133.4	83.23
		52.3				
		34.7				
	2	216.3	238.7	101.0		
		150.7				
		348.9				
	3	66.3	88.5	30.7		
		123.5				
		75.7				
	4	146.0	157.4	11.7		
		169.3				
		157.0				
1a	1	63.5	44.0	17.1	36.6	10.50
		31.3				
		37.2				
	2	29.8	29.2	9.6		
		19.3				
		38.5				
2	1	107.2	103.2	11.2	106.3	3.30
		90.5				
		111.8				
	2	87.2	109.7	27.5		
		140.4				
		101.6				
	3	114.9	105.9	10.7		
		94.0				
		108.7				
2a	1	78.3	56.2	19.3	39.3	23.93
		47.4				
		42.9				
	2	14.7	22.4	8.5		
		20.9				
		31.6				
3	1	129.1	144.1	54.3	144.1	54.30
		204.3				
		99.0				
3a	1	127.2	96.8	26.3	126.3	41.72
		81.6				
		81.6				
	2	170.8	155.8	13.0		
		147.1				
		149.5				
4	1	114.1	127.0	14.4	127.9	1.24
		142.6				
		124.4				
	2	131.0	128.8	21.9		
		149.5				
		105.8				
5	1	150.7	118.4	29.4	133.8	15.82
		93.4				
		111.0				
	2	126.2	133.2	6.6		
		139.3				
		134.0				
	3	155.7	150.0	4.9		
		147.1				
		147.1				

TABLE 12.--Raw Data for Vicker's Hardness (H_v) for Bone Pieces and Teeth (continued).

Bone #	Point #	Vicker's Hardness	Ave. Point H_v	Point H_v Std. Dev	Ave. Piece H_v	Piece H_v Std. Dev
6	1	143.7	166.5	21.5	239.1	75.20
		186.4				
		169.3				
	2	429.0	316.6	158.7		
		135.0				
		385.8				
	3	324.6	234.3	103.3		
		121.7				
		256.8				
7	1	38.1	31.9	9.7	89.5	81.41
		20.8				
		36.9				
	2	101.0	147.1	53.8		
		206.3				
		134.0				
8	1	160.9	152.7	14.4	74.4	68.19
		160.9				
		136.1				
	2	27.5	43.0	15.1		
		43.8				
		57.6				
	3	23.2	27.6	4.8		
		26.9				
		32.8				
9	1	130.0	141.9	35.2	132.5	15.77
		181.5				
		114.1				
	2	98.4	114.3	23.7		
		103.0				
		141.4				
	3	128.1	141.3	16.4		
		136.1				
		159.6				
10	1	75.7	127.9	58.8	131.6	5.26
		191.5				
		116.6				
	2	173.7	135.4	33.3		
		114.1				
		118.2				
11	1	49.4	65.6	30.1	88.9	23.77
		47.0				
		100.3				
	2	142.6	121.6	18.7		
		115.7				
		106.5				
	3	72.7	79.9	6.6		
		89.4				
		77.4				
	4	97.1	88.6	12.7		
		94.6				
		74.0				
12	1	111.0	132.5	58.5	132.5	58.50
		87.8				
		198.7				

TABLE 12.--Raw Data for Vicker's Hardness (H_v) for Bone Pieces and Teeth (continued).

Bone #	Point #	Vicker's Hardness	Ave. Point H_v	Point H_v Std. Dev	Ave. Piece H_v	Piece H_v Std. Dev
13	1	57.1	43.8	12.1	65.7	15.93
		40.9				
		33.4				
	2	53.8	64.5	17.4		
		55.1				
		84.6				
	3	76.3	74.8	3.8		
		70.7				
		75.2				
	4	93.4	79.7	12.5		
		77.0				
		68.8				
14	1	172.2	126.8	41.2	80.3	58.34
		116.6				
		91.7				
	2	146.0	133.4	11.0		
		125.3				
		129.1				
	3	28.9	19.5	8.8		
		18.0				
		11.5				
	4	41.1	41.3	2.1		
		39.2				
		43.4				
15	1	90.0	97.6	18.1	101.5	82.48
		118.2				
		84.6				
	2	173.7	219.2	50.7		
		273.8				
		210.2				
	3	33.3	48.6	16.2		
		65.6				
		47.0				
	4	31.3	40.4	13.8		
		33.6				
		56.2				
16	1	46.2	46.2	2.2	60.1	27.52
		44.0				
		48.3				
	2	105.8	91.8	21.3		
		67.3				
		102.3				
	3	51.1	72.6	26.6		
		102.3				
		64.5				
	4	29.8	29.9	1.2		
		28.7				
		31.1				

TABLE 12.–Raw Data for Vicker's Hardness (H_v) for Bone Pieces and Teeth (continued).

Bone #	Point #	Vicker's Hardness	Ave. Point H_v	Point H_v Std. Dev	Ave. Piece H_v	Piece H_v Std. Dev
17	1	46.8	52.5	17.3	111.2	43.33
		71.9				
		38.8				
	2	111.8	113.9	2.0		
		114.1				
		115.7				
	3	109.5	121.5	73.7		
		200.5				
		54.6				
	4	148.3	156.7	24.9		
		137.1				
		184.7				
18	1	396.0	252.5	141.8	140.9	85.58
		248.9				
		112.5				
	2	137.1	161.8	32.6		
		149.5				
		198.7				
	3	127.2	87.4	42.0		
		43.4				
		91.7				
	4	38.1	62.0	23.3		
		84.6				
		63.2				
20	1	35.9	32.9	2.9	31.3	2.18
		32.5				
		30.2				
	2	27.2	29.8	2.3		
		31.4				
		30.8				
20a	1	23.1	28.6	4.8	19.0	13.62
		31.8				
		30.9				
	2	8.4	9.3	1.7		
		11.3				
		8.3				
21	1	5.2	7.3	2.7	7.4	0.11
		6.3				
		10.3				
	2	6.2	7.4	1.3		
		8.8				
		7.4				
21a	1	13.7	13.8	1.9	15.2	1.93
		15.8				
		12.0				
	2	20.0	16.5	3.5		
		13.0				
		16.6				
22	1	17.7	23.7	5.2	28.1	6.19
		26.7				
		26.7				
	2	26.7	32.5	5.7		
		32.5				
		38.1				

TABLE 12.–Raw Data for Vicker's Hardness (H_v) for Bone Pieces and Teeth (continued).

Bone #	Point #	Vicker's Hardness	Ave. Point H_v	Point H_v Std. Dev	Ave. Piece H_v	Piece H_v Std. Dev
22a	1	38.1	34.4	7.1	27.7	9.45
		26.2				
		38.9				
	2	19.9	21.1	1.1		
		22.1				
		21.2				
23	1	19.2	14.9	4.1	26.8	11.09
		11.1				
		14.4				
	2	13.1	20.1	6.2		
		22.1				
		25.1				
	3	25.1	38.0	14.6		
		35.0				
		53.8				
	4	44.6	34.4	9.7		
		25.2				
		33.5				
24	1	5.3	5.1	0.9	20.8	11.66
		4.1				
		5.9				
	2	21.2	22.1	1.1		
		23.4				
		21.9				
	3	26.9	22.5	3.8		
		19.6				
		21.1				
	4	37.2	33.3	12.5		
		19.3				
		43.4				
25	1	21.3	24.3	2.8	21.2	3.50
		24.8				
		26.7				
	2	30.6	22.5	7.9		
		21.9				
		14.9				
	3	25.1	22.0	3.6		
		22.8				
		18.1				
	4	16.3	16.2	2.3		
		18.4				
		13.8				
26	1	24.2	19.5	4.4	26.3	5.72
		18.8				
		15.4				
	2	18.4	24.4	6.2		
		23.8				
		30.9				
	3	29.3	28.5	1.9		
		26.4				
		29.9				
	4	25.7	32.8	6.2		
		36.9				
		35.9				

TABLE 12.--Raw Data for Vicker's Hardness (H_v) for Bone Pieces and Teeth (continued).

Bone #	Point #	Vicker's Hardness	Ave. Point H_v	Point H_v Std. Dev	Ave. Piece H_v	Piece H_v Std. Dev
30	1	12.4	14.0	3.9	17.4	8.27
		18.5				
		11.2				
	2	17.9	15.5	2.4		
		15.5				
		13.2				
	3	10.6	10.6	0.2		
		10.8				
		10.4				
	4	31.3	29.4	1.9		
		27.6				
		29.3				
31	1	34.4	36.3	11.5	26.1	7.71
		25.8				
		48.5				
	2	29.5	25.5	4.1		
		21.3				
		25.8				
	3	21.8	17.5	4.3		
		17.6				
		13.2				
	4	24.8	24.9	1.9		
		26.8				
		22.9				
32	1	23.4	24.9	1.3	17.0	5.93
		25.7				
		25.7				
	2	17.4	16.0	1.3		
		15.9				
		14.9				
		17.3	16.6	2.9		
	3	13.5				
		19.1				
	4	8.8	10.5	1.5		
		11.7				
		11.1				
33	1	12.6	12.6	0.3	17.8	5.09
		12.2				
		12.8				
	2	16.8	24.7	8.1		
		33.0				
		24.4				
	3	16.1	17.6	1.4		
		17.7				
		19.0				
	4	16.9	16.3	0.6		
		15.8				
		16.2				

TABLE 12.--Raw Data for Vicker's Hardness (H_v) for Bone Pieces and Teeth (continued).

Bone #	Point #	Vicker's Hardness	Ave. Point H_v	Point H_v Std. Dev	Ave. Piece H_v	Piece H_v Std. Dev
34	1	24.5	23.7	1.0	17.2	5.27
		22.6				
		23.9				
	2	13.6	13.6	0.5		
		13.0				
		14.0				
	3	14.2	12.3	1.8		
		10.6				
		12.2				
	4	17.0	19.3	2.2		
		21.3				
		19.6				
35	1	14.3	11.7	2.3	17.8	4.14
		10.9				
		9.9				
	2	25.4	23.0	3.0		
		19.6				
		24.0				
	3	19.9	20.4	0.5		
		20.2				
		21.0				
	4	20.8	20.1	1.0		
		19.0				
		20.5				
	5	17.7	15.0	2.4		
		13.1				
		14.1				
	6	18.2	16.6	1.5		
		16.4				
		15.2				
36	1	18.2	18.1	1.3	19.0	7.55
		16.7				
		19.2				
	2	15.2	14.0	1.1		
		13.0				
		13.8				
	3	24.0	18.1	5.1		
		15.4				
		15.0				
	4	11.7	15.2	4.4		
		13.8				
		20.1				
	5	15.1	14.6	1.0		
		15.4				
		13.4				
	6	29.0	34.0	13.9		
		23.2				
		49.7				
40	1	56.2	54.4	2.1	52.4	4.07
		52.1				
		54.9				
	2	47.7	47.7	0.9		
		48.5				
		46.8				
	3	57.1	55.0	3.8		
		50.6				
		57.4				

TABLE 12.--Raw Data for Vicker's Hardness (H_v) for Bone Pieces and Teeth (continued).

Bone #	Point #	Vicker's Hardness	Ave. Point H_v	Point H_v Std. Dev	Ave. Piece H_v	Piece H_v Std. Dev
41	1	52.1	67.4	17.3	66.0	1.93
		86.2				
		63.9				
	2	63.5	64.6	8.4		
		73.6				
		56.8				
42	1	27.5	36.7	10.8	49.5	20.74
		48.5				
		34.2				
	2	70.4	76.7	18.7		
		97.7				
		61.9				
	3	46.4	54.3	7.5		
		55.1				
		61.3				
	4	30.2	30.3	8.5		
		38.9				
		21.9				
43	1	82.1	65.6	19.0	43.1	19.08
		70.0				
		44.8				
	2	52.6	47.0	5.6		
		41.3				
		47.2				
	3	21.6	19.4	3.2		
		15.6				
		20.8				
	4	44.6	40.6	5.0		
		35.0				
		42.1				
44	1	39.1	39.9	2.4	27.8	8.21
		38.0				
		42.5				
	2	31.2	26.3	5.2		
		20.9				
		26.7				
	3	15.3	22.9	6.8		
		25.2				
		28.3				
	4	20.5	22.2	1.6		
		23.7				
		22.6				
45	1	22.6	37.4	13.9	19.6	11.88
		39.4				
		50.1				
	2	15.8	15.0	0.9		
		15.2				
		14.1				
	3	15.3	13.4	1.9		
		11.6				
		13.4				
	4	11.9	12.6	2.0		
		14.9				
		11.1				

TABLE 12.--Raw Data for Vicker's Hardness (H_v) for Bone Pieces and Teeth (continued).

Bone #	Point #	Vicker's Hardness	Ave. Point H_v	Point H_v Std. Dev	Ave. Piece H_v	Piece H_v Std. Dev
46	1	28.4	31.5	5.1	25.7	4.86
		28.6				
		37.4				
	2	20.8	19.6	1.3		
		18.2				
		19.9				
	3	24.2	26.4	5.5		
		22.4				
		32.6				
	4	27.8	25.2	5.8		
		29.2				
		18.5				
47	1	36.5	27.3	8.0	45.1	21.62
		23.9				
		21.6				
	2	36.6	37.9	11.8		
		50.4				
		26.8				
	3	28.2	38.4	11.5		
		50.8				
		36.2				
	4	89.4	76.6	16.3		
		58.2				
		82.1				
50	1	82.1	67.4	12.8	62.2	9.09
		60.0				
		60.0				
	2	46.4	51.7	15.2		
		39.7				
		68.8				
	3	72.3	67.4	5.1		
		62.2				
		67.7				
51	1	33.9	33.0	1.9	27.5	7.79
		30.8				
		34.3				
	2	24.0	22.0	2.0		
		20.2				
		21.7				
52	1	123.5	148.6	73.9	117.3	28.93
		231.8				
		90.5				
	2	114.1	135.2	22.9		
		132.0				
		159.6				
	3	86.2	93.2	13.5		
		108.7				
		84.6				
	4	61.6	92.2	28.3		
		97.7				
		117.4				

TABLE 12.–Raw Data for Vicker's Hardness (H_v) for Bone Pieces and Teeth (continued).

Bone #	Point #	Vicker's Hardness	Ave. Point H_v	Point H_v Std. Dev	Ave. Piece H_v	Piece H_v Std. Dev
53	1	83.1	81.6	4.9	60.9	25.72
		85.6				
		76.1				
	2	68.8	66.7	3.1		
		63.2				
		68.1				
	3	72.3	71.8	11.5		
		83.1				
		60.0				
	4	23.1	23.5	2.5		
		21.2				
		26.1				
54	1	56.2	82.4	24.4	86.6	14.99
		104.4				
		86.7				
	2	68.5	70.3	7.3		
		76.3				
		64.2				
	3	94.6	87.3	6.8		
		81.1				
		86.2				
	4	126.2	106.4	17.2		
		97.1				
		95.8				
55	1	61.3	66.7	4.7	37.2	21.80
		70.0				
		68.8				
	2	26.5	21.1	5.8		
		14.9				
		21.9				
	3	22.4	20.3	2.2		
		17.9				
		20.7				
	4	36.8	40.6	3.7		
		44.2				
		40.7				
56	1	17.5	18.6	2.6	35.0	20.84
		21.6				
		16.8				
	2	74.0	49.6	24.2		
		49.2				
		25.6				
	3	53.8	56.1	7.6		
		64.5				
		49.9				
	4	17.0	15.6	2.3		
		12.9				
		16.8				

TABLE 12.--Raw Data for Vicker's Hardness (H_v) for Bone Pieces and Teeth (continued).

Bone #	Point #	Vicker's Hardness	Ave. Point H_v	Point H_v Std. Dev	Ave. Piece H_v	Piece H_v Std. Dev
57	1	81.6	73.4	8.4	66.7	16.80
		64.9				
		73.6				
	2	57.1	56.7	5.4		
		61.9				
		51.1				
	3	88.3	87.0	10.2		
		76.1				
		96.5				
	4	37.1	49.6	12.4		
		61.9				
		49.9				
60	1	23.9	18.1	5.5	16.5	1.47
		17.4				
		13.0				
	2	15.8	17.4	1.6		
		17.3				
		19.0				
	3	14.4	15.3	2.8		
		18.4				
		13.1				
	4	10.9	15.2	4.4		
		19.8				
		14.9				
61	1	64.9	84.0	22.5	78.0	8.50
		78.3				
		108.7				
	2	56.2	72.0	13.0		
		73.6				
		84.1				
62	1	46.8	53.8	6.6	66.4	17.77
		60.0				
		54.6				
	2	71.1	78.9	36.0		
		47.4				
		118.2				
63	1	74.4	59.1	14.9	60.1	1.45
		44.6				
		58.2				
	2	53.6	61.1	6.7		
		63.5				
		66.3				
64	1	89.4	65.9	23.2	70.4	6.34
		43.1				
		65.2				
	2	79.7	74.9	5.3		
		69.2				
		75.7				
65	1	28.8	22.2	7.0	18.5	5.17
		22.8				
		14.9				
	2	15.6	14.8	1.0		
		15.3				
		13.7				

TABLE 12.–Raw Data for Vicker's Hardness (H_v) for Bone Pieces and Teeth (continued).

Bone #	Point #	Vicker's Hardness	Ave. Point H_v	Point H_v Std. Dev	Ave. Piece H_v	Piece H_v Std. Dev
66	1	11.4	12.1	0.7	16.9	9.67
		12.8				
		12.2				
	2	10.1	31.4	25.8		
		24.0				
		60.0				
	3	10.4	11.9	1.5		
		11.8				
		13.5				
	4	10.6	12.1	2.1		
		11.0				
		14.5				
67	1	67.7	58.9	32.1	31.3	18.68
		23.3				
		85.6				
	2	38.0	26.8	9.8		
		22.7				
		19.8				
	3	18.3	18.8	1.0		
		19.9				
		18.2				
	4	22.8	20.8	1.8		
		19.2				
		20.3				
70	1	69.2	76.1	16.8	72.8	11.78
		63.9				
		95.2				
	2	59.7	59.7	5.1		
		54.6				
		64.9				
	3	89.4	82.6	7.3		
		74.8				
		83.6				
71	1	57.1	52.3	4.2	48.5	8.43
		49.4				
		50.4				
	2	35.5	38.8	3.6		
		38.3				
		42.7				
	3	49.9	54.3	4.2		
		54.9				
		58.2				
72	1	46.4	52.8	12.3	51.2	13.81
		67.0				
		45.0				
	2	36.0	31.2	6.1		
		26.1				
		29.5				
	3	68.1	60.5	12.4		
		67.3				
		46.2				
	4	50.1	60.2	11.8		
		57.4				
		73.1				

TABLE 12.–Raw Data for Vicker's Hardness (H_v) for Bone Pieces and Teeth (continued).

Bone #	Point #	Vicker's Hardness	Ave. Point H_v	Point H_v Std. Dev	Ave. Piece H_v	Piece H_v Std. Dev
73	1	45.8	48.5	6.3	56.4	9.61
		55.7				
		44.0				
	2	62.9	64.8	14.5		
		51.3				
		80.2				
	3	69.2	65.1	9.6		
		54.1				
		71.9				
	4	44.2	47.4	3.5		
		51.1				
		47.0				
74	1	28.5	25.8	4.0	19.7	4.68
		27.7				
		21.2				
	2	21.4	20.8	5.9		
		26.4				
		14.7				
	3	16.0	17.2	3.2		
		20.9				
		14.7				
	4	14.5	15.1	2.9		
		18.2				
		12.6				
75	1	12.3	9.7	2.3	25.7	13.09
		7.9				
		9.0				
	2	33.0	29.9	3.8		
		31.1				
		25.8				
	3	42.7	40.8	1.6		
		39.9				
		39.9				
	4	22.6	22.3	2.7		
		19.5				
		24.8				
76	1	22.5	21.8	2.4	42.2	16.78
		23.7				
		19.1				
	2	63.2	61.2	2.2		
		58.8				
		61.6				
	3	51.3	48.7	18.0		
		65.2				
		29.6				
	4	33.1	37.3	4.2		
		41.4				
		37.2				

TABLE 12.--Raw Data for Vicker's Hardness (H_v) for Bone Pieces and Teeth (continued).

Bone #	Point #	Vicker's Hardness	Ave. Point H_v	Point H_v Std. Dev	Ave. Piece H_v	Piece H_v Std. Dev
77	1	42.7	39.6	4.9	46.2	11.97
		33.9				
		42.1				
	2	35.9	32.8	3.2		
		29.5				
		33.1				
	3	57.1	58.1	7.4		
		51.3				
		65.9				
	4	54.9	54.3	2.3		
		56.2				
		51.8				
80	1	61.6	60.0	3.6	62.8	25.32
		62.5				
		56.0				
	2	76.1	89.4	12.8		
		101.6				
		90.5				
	3	40.4	39.0	1.6		
		39.4				
		37.2				
81	1	50.6	55.0	4.4	47.5	6.50
		59.4				
		54.9				
	2	31.7	43.4	10.6		
		52.3				
		46.2				
	3	42.5	44.1	4.8		
		49.4				
		40.2				
82	1	53.6	49.6	3.4	74.5	27.82
		47.2				
		48.1				
	2	53.3	57.8	4.8		
		62.9				
		57.4				
	3	184.7	112.0	63.0		
		76.1				
		75.2				
	4	69.2	78.6	14.0		
		94.6				
		71.9				
83	1	12.6	12.8	0.8	33.4	15.21
		12.1				
		13.7				
	2	26.4	31.0	4.0		
		33.5				
		33.1				
	3	48.3	45.6	2.4		
		44.6				
		43.8				
	4	44.0	44.1	2.6		
		41.6				
		46.8				

TABLE 12.--Raw Data for Vicker's Hardness (H_v) for Bone Pieces and Teeth (continued).

Bone #	Point #	Vicker's Hardness	Ave. Point H_v	Point H_v Std. Dev	Ave. Piece H_v	Piece H_v Std. Dev
84	1	25.2	38.9	11.9	19.2	13.14
		47.2				
		44.2				
	2	12.1	11.6	0.6		
		10.9				
		11.9				
	3	14.6	13.8	1.2		
		14.3				
		12.5				
	4	14.0	12.6	1.7		
		13.1				
		10.7				
85	1	57.4	54.2	4.0	52.8	11.27
		55.4				
		49.7				
	2	31.3	41.8	9.6		
		43.8				
		50.1				
	3	48.1	47.3	1.5		
		48.1				
		45.6				
	4	74.4	67.8	7.1		
		68.8				
		60.3				
87	1	28.8	40.0	13.2	59.6	18.12
		36.6				
		54.6				
	2	73.6	62.9	12.2		
		49.7				
		65.6				
	3	90.0	75.8	12.6		
		71.5				
		65.9				
		30.5				
*manl	1	262.3	266.1	4.4	251.9	20.08
		270.9				
		265.1				
	2	198.7	237.7	51.4		
		218.4				
		295.9				
*manc	1	155.7	167.7	10.9	199.1	44.40
		176.8				
		170.8				
	2	259.5	230.5	63.0		
		273.8				
		158.3				
*manp	1	259.5	271.2	13.6	240.6	43.23
		268.0				
		286.1				
	2	159.6	210.0	43.7		
		236.5				
		234.1				
*maxi	1	302.7	241.8	64.8	233.6	11.58
		173.7				
		248.9				
	2	214.3	225.4	43.9		
		188.1				
		273.8				

TABLE 12.--Raw Data for Vicker's Hardness (H_v) for Bone Pieces and Teeth (continued).

Bone #	Point #	Vicker's Hardness	Ave. Point H_v	Point H_v Std. Dev	Ave. Piece H_v	Piece H_v Std. Dev
*maxc	1	225.0	254.6	25.7	268.5	19.64
		268.0				
		270.9				
	2	295.9	282.4	15.7		
		265.1				
		286.1				
*maxp	1	268.0	274.5	19.0	276.2	2.51
		295.9				
		259.5				
	2	279.9	278.0	25.7		
		302.7				
		251.5				

*mani- mandibular incisor, *manc- mandibular canine,* manp- mandibular premolar
*maxi- maxillary incisor, *maxc- maxillary canine, *maxp- maxillary premolar

TABLE 13.–Raw Data for Radiointensity Values for Cortical Bone and Teeth.

Bone #	Ave. Vol. (ml)	Est Vol. (ml)	Ave. Inten. (Hounsfields)	STD Dev.
1	0.1	0.27	3075.04	443.15
1a	0.1	0.1	2077.54	316.69
2	0.5	0.5	3113.39	405.07
2a	0.1	0.1	2164.56	244.14
3	0.15	0.05	2396.78	260.4
3a	0.05	0.15	2515.05	168.88
4	0.25	0.1	2301.5	521.79
5	0.5	0.5	2064.31	369.87
6	0.4	0.4	2277.59	241.19
7	0.25	0.25	2593.71	252.2
8	0.7	0.7	2352.11	281.27
9	1	1.6	2621.25	373.27
10	1	1.1	2336.66	444.87
11	0.7	0.7	2605.9	310.19
12	0.1	0.1	2816.88	260.08
13	2.9	2.9	2726.66	304.49
14	2.6	2.6	2550.26	384.88
15	1.6	2.47	2844.84	240.34
16	1.4	2.2	2932.35	270.95
17	0.5	0.5	2914.85	284.37
18	1	1	2629.72	266.55
20	1.1	1.13	2840.57	254.47
20a	0.8	0.77	2827.59	296.11
21	1	1	2860.18	243.88
21a	0.6	0.94	2865.37	259.72
22	0.9	0.87	2826.01	260.12
22a	1.1	1.91	2838.47	260.91
23	1.6	1.6	2819.37	306.47
24	2	2	2705.48	305.72
25	1.5	1.54	2827.61	251.93
26	1.9	2.04	2785.22	253.71
30	1.9	1.93	2809.17	261.14
31	1.4	1.4	2828.51	251.16
32	2	2	2766.44	348.37
33	1.8	1.8	2697.22	338.76
34	1.7	1.7	2817.29	269.15
35	1.8	1.82	2896.55	281.07
36	2.3	2.32	2889.28	270.58
40	0.5	0.5	2947.2	322.13
41	0.1	0.1	2410.37	311.66
42	1.4	1.4	2880.87	264.78
43	1.7	1.73	2355.63	480.72
44	0.8	0.8	2675.25	363.43
45	1.4	1.4	2597.69	332.85
46	2	2	2838.13	391.56
47	1.6	1.57	2358.73	362.14
50	0.5	0.51	3021.78	339.68
51	0.2	0.2	2381.94	350.3
52	1.1	1.1	2874.56	258.83
53	1.6	1.6	2663.24	342.95
54	1.2	1.2	2779.49	375
55	1	1.03	2748.01	281.16
56	1	1	2868.82	321.91
57	0.8	0.8	2698.56	280.59
60	0.8	0.8	1946.71	369.54
61	0.2	0.2	2623.89	184.86

TABLE 13.—Raw Data for Radiointensity Values for Cortical Bone and Teeth (continued)

Bone #	Ave. Vol. (ml)	Est Vol. (ml)	Ave Inten. (Hounsfields)	STD Dev
62	0.4	0.37	2043.97	220.2
63	0.1	0.26	3006.35	310.81
64	0.2	0.44	2960.98	299.95
65	0.2	0.2	2224.69	461.23
66	0.5	0.54	2949.83	289.63
67	0.5	0.56	2915.07	281.36
70	0.7	0.7	2771.15	319.3
71	1.7	1.7	2689.68	370.55
72	2.4	2.4	2732.14	465.81
73	1.5	1.47	2845.38	389.3
74	1.1	1.1	2908.53	346.24
75	1.7	1.7	2565.34	570.9
76	0.6	0.63	2996.51	306.13
77	1	1	2797.57	393.45
80	0.5	0.5	2296.08	422.26
81	3.4	3.4	2690.54	543.4
82	1.2	3.4	2457.17	563.33
83	1.2	1.2	2642.75	518.72
84	0.7	0.7	2376.22	522.32
85	2	2	2469.04	617.5
87	0.7	0.7	3027.83	355.47
*mani	0.6	0.71	3247.27	340.44
*manc	0.6	0.6	3213.97	393.92
*manp	0.5	0.37	3104.73	609.1
*maxi	0.5	0.54	3299.28	325.91
*maxc	0.4	0.69	3249.51	317.91
*maxp	0.6	0.6	3066.07	577.79

*mani- mandibular incisor, *manc- mandibular canine, *manp- mandibular premolar
*maxi- maxillary incisor, *maxc- maxillary canine, *maxp- maxillary premolar

BIBLIOGRAPHY

Akkus O, Polyakova-Akkus A, Adar F, Schaffler MB. 2003. Aging of microstructural compartments in human compact bone. J Bone Miner Res 18:1012-9.

Arbel G. 1993. A finite element structural model of the facial skeleton. The relationship of the architecture of the face to the masticatory system. PhD Thesis, Tel Aviv University, Israel.

Arendts FJ, Sigolotto C. 1990. Mechanical characteristics of the human mandible, and investigation of the "in-vivo" reaction of the compact bone: a contribution to the description of the biomechanics of the mandible-part II. Biomed Tech 35:123-130.

Ashman RB, van Buskirk WC. 1987. The elastic properties of a human mandible. Adv Dent Res 1:64-67.

Ashman RB, Corin JD, Turner CH. 1987. Elastic properties of cancellous bone: Measurement by an ultrasonic technique. J Biomech 20:979-986.

Broadbent BH Sr. 1931. A new x-ray technique and its application to orthodontia. Angle Orthod 1:45-66.

Bumerraj S & Katz JL. 2001. SAM study of human cortical and trabecular bone. Biomed Eng 29:1034-1042.

Cattaneo P, Dalstra M, Melsen B. 2003. The transfer of occlusal forces through the maxillary molars: A finite element study. Am J Orthod Dentofacial Orthop 123:367-73.

Couly JD. 1976. The Mechanical Adaptation of Bones. Princeton University Press, Princeton, NJ.

Currey JD, Brear K. 1990. Hardness. Young's modulus and yield stress in mammalian mineralized tissue. J Mat Sci Mater Med 1:14-20.

Dabney CL, Dechow PC. 2003. Variations in cortical material properties throughout the human dentate mandible. Am J Phys Anthropol 120(3):252-77.

Dean D, Hans MG, Bookstein FL, Broadbent BH Jr., Subtramanyan K. 2000. Three Dimensional Bolton-Brush Growth Study Landmark Data: Ontogeny and Sexual Dimorphism of the Bolton Standards Cohort. Cleft Palate-Craniofac J 37:145-156.

Dean D, Mullen R, Katz JL, Min J, Totonchi A, Ahmad Y, Wolfe M, Armanazi Y, Hans MG. The construction of a biomechanical model of the cranium as the basis for a treatment simulator. In JA Mc Namara, Clinical Orthodontics and Information Technology: The Nuts and Bolts of Bytes and Bites. Ann Arbor: University of Michigan Press, in press.

Dechow PC, Nail GA, Dabney CL, Ashman RB. 1993. Elastic properties of human supraorbital and mandibular bone. Am J Phys Anthropol 90:291-306.

Gibson LS, Ashby MF. 1997. Cellular Fluids. Ed.2 Cambridge University Press, Cambridge.

Gross MD, Arbel G, Hershkovitz I. 2001. Three-dimensional finite element analysis of the facial skeleton on simulated occlusal loading. J Oral Rehab 28:684-694.

Hans MG, Palomo JM, Dean D, Min J-K, Han S, Ganne J. 2001. Three dimensional cephalometry: The CWRU method. Seminars in Orthodontics 7:233-243.

Huja S, Katona T, Moore B, Roberts W. 1998. Microhardness and Anisotropy of the Vital Osseous Interface and Endosseous Implant Supporting Bone. J Orthop Res 16:54-60.

Hylander WL. 1975. The human mandible: level or link? Am J Phys Anthropol 43, 227.

Hylander WL. 1984. Stress and strain in the mandibular symphysis of primates: a test of competing hypotheses. Am J Physl Anthropol 64,1-46.

Hylander WL. 1985. Mandibular function and biomechanical stress and scaling. American Zoologist, 25, 315-376.

Hylander WL, Picq PG, Johnson KR. 1991. Masticatory stress hypotheses and the supraorbital region of primates. Am J Phys Anthropol 86,1-36.

Jafari A, Shetty K, Kumar M. 2003. Study of the stress distribution and displacement of various craniofacial structures following application of transverse orthopedic forces- A three-dimensional FEM study. Angle Orthod 73:12-20.

Jung T, Dean D, Mullen R, Min KJ, Ahmad Y, Totonchi A, Kondapalli S, Katz JL, Hans MG. Nondestructive methods for the assembly of a craniofacial finite element model. AADR/CADR Annual Meeting, San Antonio, Texas, March 12-15, 2003.

Keenan M, Hegsted M, Jones K, Delany J, Kime J, Melancon L, Tulley R, Hong K. 1997. Comparison of bone density measurement techniques: DXA and Archimedes' principle. J Bone Miner Res 12(11):1903-1907.

Keyak JH, Fourkas MG, Meagher JM, Skinner HB. Validation of an automated method of three-dimensional finite element modeling of bone. J Biomed Eng 15(6):505-9.

Klein C. 1989. Minerals and Rocks: Exercises in Crystallography, Mineralogy, and Hand Specimen Petrology. Wiley, New York.

Lai K, Rencken M, Drinkwater B, Chestnut C. 1993. Site of bone density measurement may affect therapy decision. Calcif Tissue Int 53:225-228.

Lettry S, Seedhom BB, Berry E, Cuppone M. 2003. Quality assessment of the cortical bone of the human mandible. Bone 32:35-44.

Meijer HJA, Starmans FJM, Bosman F, Steen WHA. 1993. A comparison of three finite element models of an edentulous mandible provided with implants. J Oral Rehab 20:147-57.

Mullen RL, Rudderman RH. 1992. Biomechanics of the facial skeleton. Clin Plast Surg 19:11-29.

Peterson J, Dechow PC. 2002. Material Properties of the Inner and Outer Cortical Tables of the Human Parietal Bone. Anat Rec 268:7-15.

Sato M. 1995. Comparative x-ray densitometry of bones from ovarietomized rats. Bone 17:157S-162S.

Sicher H, Tandler J. 1928. Anatomie Fur Zahnartzte. Springer, Berlin.

Sievanen H, Kannus P, Jarvinen M. 1994. Precision of measurement by dual-energy absorptiometry of bone mineral density and content in rat hindlimb in vitro. J Bone Miner Res 9:473-478.

Snyder S & Schneider E. 1991. Estimation of mechanical properties of cortical bone by computed tomography. J Orthop Res 9:422-431.

Subramanyan K, Dean D. 2000. Production of Average 3D Anatomical Surfaces. Med Image Anal 4:317-334.

Tappen NC. 1953. A Functional analysis of the facial skeleton with split line technique. Am J Phys Anthropol 11,503.

Turner CH, Eich M. 1991. Ultrasonic velocity as a predictor of strength in bovine cancellous bone. Calcif Tissue Int 49:116-119.

Ulrich D, van Rietbergen B, Laib A, Ruegseeger P. 1999. Load transfer analysis of the distal radius from in-vivo high resolution CT-imaging. J Biomech 32:821-828.

Wirtz DC, Schiffers N, Pandorf T, Radermacher K, Weichert D, Forst R. 2000. Critical evaluation of known bone material properties to realize anisotropic FE-simulation of the proximal femur. J Biomech 33:1325-1330.

Yoon HS, Katz JL. 1976. Ultrasonic wave propagation in human cortical bone II. Measurements of elastic properties and microhardness. J Biomech 9:459-464.

Zioupos P, Currey J. 1998. Changes in the stiffness, strength, and toughness of human cortical bone with age. Bone 22:57-66.



8 95 CW TH 5493
03/04 00-104-07 GBC